CHAPTER

1

INTRODUCTION TO CONCEPTS AND SYSTEMS

Prior to the 1960s our view of the earth and the universe was restricted to observations and photographs using visible light. Distant views were obtained only from aircraft and telescopes. Today the science of remote sensing provides instruments that view our universe at wavelengths far greater than those of visible light. The instruments are deployed in satellites and aircraft to record images of the earth and solar system that can be digitally analyzed with our personal computers to provide information on a wide range of topics. Some of these include the global environment, land use, renewable and nonrenewable resources, natural hazards, and the geology of Venus.

In this book *remote sensing* is defined as the science of

- acquiring,
- processing, and
- interpreting

images, and related data, obtained from aircraft and satellites that record the interaction between matter and electromagnetic radiation. *Acquiring* images refers to the technology employed, such as an electro-optical scanning system. *Processing* refers to the procedures that convert the raw data into images. *Interpreting* the images is, in my opinion, the most important step because it converts an image into information that is meaningful and valuable for a wide range of users. The *interaction between matter and electromagnetic energy* is determined by

- the physical properties of the matter, and
- the wavelength of electromagnetic energy that is remotely sensed.

A later section in this chapter describes the various wavelength regions and the types of interactions.

The term *remote sensing* refers to methods that employ electromagnetic energy, such as light, heat, and radio waves, as the means of detecting and measuring target characteristics. Underwater surveys that use pulses of sonic energy for imaging (*sonar*) are considered a remote sensing method. The science of remote sensing excludes geophysical methods such as electrical, magnetic, and gravity surveys that measure force fields rather than electromagnetic radiation.

Aerial photography is the original form of remote sensing and remains a widely used method. Interpretations of aerial photographs have led to the discovery of many oil and mineral deposits. These successes, using only the visible region of the electromagnetic spectrum, suggested that additional discoveries could be made by using other wavelength regions. In the 1960s, technology was developed to acquire images in the infrared (IR) and microwave regions, which greatly expanded the scope and applications of remote sensing. The development and deployment of manned and unmanned earth satellites began in the 1960s and provided an orbital vantage point for acquiring images of the earth. For a review of the history of remote sensing, see Fischer and others (1975). Most remote sensing data, except for aerial photographs, are now acquired in digital format and processed by computers to produce images for interpretation.

This chapter introduces the basic physical concepts and the imaging systems that are employed in remote sensing. Subsequent chapters describe major types of remote sensing and are followed by chapters that describe applications of the technology.

Table 1-1 Metric nomenclature for distance

Unit	*Symbol*	*Equivalent*
Kilometer	km	1000 m = 10^3 m
Meter[a]	m	1.0 m = 10^0 m
Centimeter	cm	0.01 m = 10^{-2} m
Millimeter	mm	0.001 m = 10^{-3} m
Micrometer[b]	μm	0.000001 m = 10^{-6} m
Nanometer	nm	10^{-9} m

[a]Basic unit

[b]Formerly called micron (μ).

UNITS OF MEASURE

This book employs the metric system with the following standard units and abbreviations:

meter	m
second	sec
kilogram	kg
gram	g
radian	rad
hertz	Hz
watt	W

Distance is expressed in the multiples and fractions of meters shown in Table 1-1. Where appropriate for clarity, English units for distance will be used, with metric equivalents shown in parentheses.

Frequency (ν) is the number of wave crests passing a given point in a specified period of time. Frequency was formerly expressed as "cycles per second," but today we use *hertz* (Hz) as the unit for a frequency of one cycle per second. The terms for designating frequencies are shown in Table 1-2.

Temperature is given in degrees Celsius (°C) or in degrees Kelvin (°K). (The Kelvin scale is also known as the *absolute temperature scale.*) A temperature of 273°K is equivalent to 0°C. (The metric system omits the degree symbol for Kelvin temperatures; however, the letter K is also used to designate other constants; so °K is used in this text.) A few temperatures commonly given in degrees Fahrenheit (°F) will remain in that scale where conversion to degrees Celsius is inconvenient.

In fractional statements, units in the denominator are identified by a fractional superscript. For example, the property called *thermal inertia (P)* for a particular rock type is expressed as

$$P = 0.53 \text{ cal} \cdot \text{cm}^{-2} \cdot \text{sec}^{-1/2} \cdot {}^\circ\text{C}^{-1}$$

This expression means that for the particular rock type, thermal inertia P equals 0.53 calories per square centimeter per second to the square root per degree Celsius.

Table 1-2 Terms used to designate frequencies

Unit	*Symbol*	*Frequency, cycles • sec^{-1}*
Hertz	Hz	1
Kilohertz	kHz	10^3
Megahertz	MHz	10^6
Gigahertz	GHz	10^9

ELECTROMAGNETIC ENERGY

Electromagnetic energy refers to all energy that moves with the velocity of light in a harmonic wave pattern. A harmonic pattern consists of waves that occur at equal intervals in time. The wave concept explains how electromagnetic energy propagates (moves), but this energy can only be detected as it interacts with matter. In this interaction, electromagnetic energy behaves as though it consists of many individual bodies called *photons* that have such particle-like properties as energy and momentum. When light bends (refracts) as it propagates through media of different optical densities, it is behaving like waves. When a light meter measures the intensity of light, however, the interaction of photons with the light-sensitive photodetector produces an electrical signal that varies in strength proportional to the number of photons. Suits (1983) describes the characteristics of electromagnetic energy that are significant for remote sensing.

Properties of Electromagnetic Waves

Electromagnetic waves can be described in terms of their velocity, wavelength, and frequency. All electromagnetic waves travel at the same velocity (c). This velocity is commonly referred to as the *speed of light,* since light is one form of electromagnetic energy. For electromagnetic waves moving through a vacuum, $c = 299{,}793 \text{ km} \cdot \text{sec}^{-1}$ or, for practical purposes, $c = 3 \times 10^8 \text{ m} \cdot \text{sec}^{-1}$.

The *wavelength* (λ) of electromagnetic waves is the distance from any point on one cycle or wave to the same position on the next cycle or wave. The *micrometer* (μm) is a convenient unit for designating wavelength of both visible and IR radiation. In order to avoid decimal numbers, optical scientists commonly employ nanometers (nm) for measurements of very short wavelengths, such as visible light.

Unlike velocity and wavelength, which change as electromagnetic energy is propagated through media of different den-

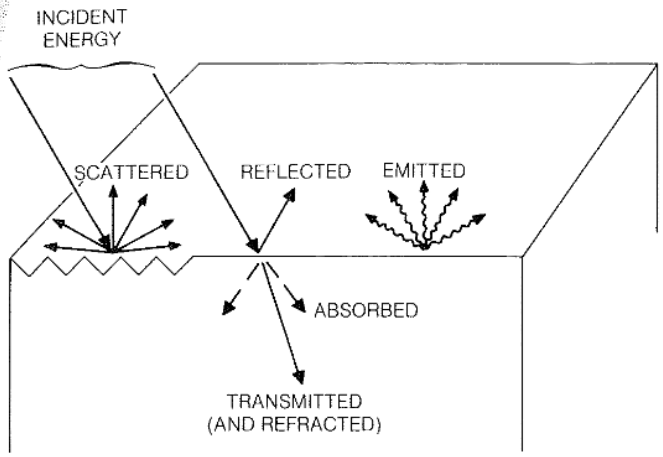

Figure 1-1 Interaction processes between electromagnetic energy and matter.

sities, frequency remains constant and is therefore a more fundamental property. Electronic engineers use frequency nomenclature for designating radio and radar energy regions. This book uses wavelength rather than frequency to simplify comparisons among all portions of the electromagnetic spectrum. Velocity (c), wavelength (λ), and frequency (ν) are related by

$$c = \lambda\nu \tag{1-1}$$

Interaction Processes

Electromagnetic energy that encounters matter, whether solid, liquid, or gas, is called *incident* radiation. Interactions with matter can change the following properties of the incident radiation: intensity, direction, wavelength, polarization, and phase. The science of remote sensing detects and records these changes. We then interpret the resulting images and data to determine the characteristics of the matter that interacted with the incident electromagnetic energy.

During interactions between electromagnetic radiation and matter, mass and energy are conserved according to basic physical principles. Figure 1-1 illustrates the five common results of these interactions. The incident radiation may be

1. *Transmitted*, that is, passed through the substance. Transmission of energy through media of different densities, such as from air into water, causes a change in the velocity of electromagnetic radiation. The ratio of the two velocities is called the *index of refraction (n)* and is expressed as

$$n = \frac{c_a}{c_s} \tag{1-2}$$

where c_a is the velocity in a vacuum and c_s is the velocity in the substance.

2. *Absorbed*, giving up its energy largely to heating the matter.
3. *Emitted* by the substance, usually at longer wavelengths, as a function of its structure and temperature.
4. *Scattered*, that is, deflected in all directions. Surfaces with dimensions of *relief*, or roughness, comparable to the wavelength of the incident energy produce scattering. Light waves are scattered by molecules and particles in the atmosphere whose sizes are similar to the wavelengths of light.
5. *Reflected*, that is, returned from the surface of a material with the angle of reflection equal and opposite to the angle of incidence. Reflection is caused by surfaces that are smooth relative to the wavelength of incident energy. *Polarization*, or direction of vibration, of the reflected waves may differ from that of the incident wave.

Emission, scattering, and reflection are called *surface phenomena* because these interactions are determined primarily by properties of the surface, such as color and roughness. Transmission and absorption are called *volume phenomena* because they are determined by the internal characteristics of matter, such as density and conductivity. The particular combination of surface and volume interactions with any particular material depend on both the wavelength of the electromagnetic radiation and the specific properties of that material.

These interactions between matter and energy are recorded on remote sensing images, from which one may interpret the characteristics of matter. Individual interaction mechanisms are described more completely in later chapters. For example, scattering of light by the atmosphere is described in Chapter 2. Absorbed and emitted thermal IR energy are described in Chapter 5. Scattering of radar energy by surfaces is described in Chapter 6.

ELECTROMAGNETIC SPECTRUM

The *electromagnetic spectrum* is the continuum of energy that ranges from meters to nanometers in wavelength, travels at the speed of light, and propagates through a vacuum such as outer space. All matter radiates a range of electromagnetic energy such that the peak intensity shifts toward progressively shorter wavelengths with increasing temperature of the matter.

Wavelength Regions and Bands

Figure 1-2 shows the electromagnetic spectrum, which is divided on the basis of wavelength into *regions* described in Table 1-3. The electromagnetic spectrum ranges from the very short wavelengths of the gamma-ray region (measured in fractions of nanometers) to the long wavelengths of the radio region (measured in meters). The horizontal scale in Figure 1-2 is logarithmic in order to portray adequately the shorter wavelengths. Notice that the visible region (0.4 to 0.7 μm) occupies only a small portion of the spectrum. Energy reflected from the

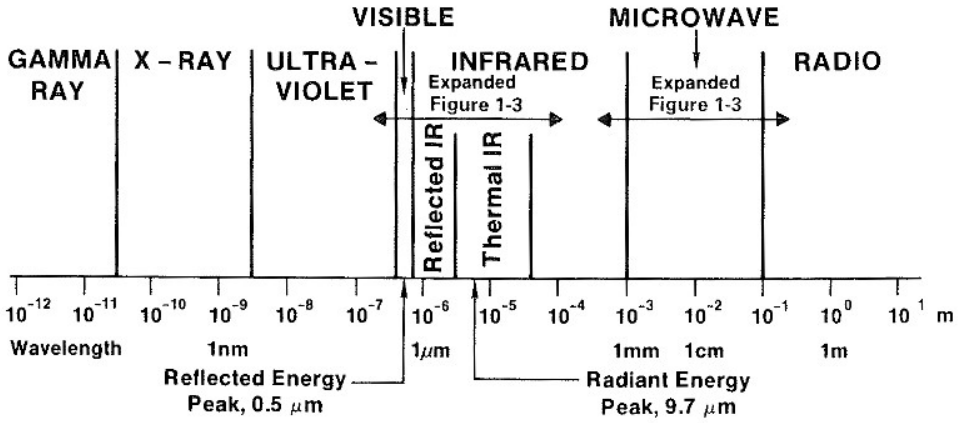

Figure 1-2 Electromagnetic spectrum. Expanded versions of the visible, infrared, and microwave regions are shown in Figure 1-3.

Table 1-3 Electromagnetic spectral regions

Region	*Wavelength*	*Remarks*
Gamma-ray region	< 0.03 nm	Incoming radiation completely absorbed by the upper atmosphere and not available for remote sensing.
X-ray region	0.03 to 30 nm	Completely absorbed by the atmosphere. Not employed in remote sensing.
Ultraviolet region	0.03 to 0.4 μm	Incoming wavelengths less than 0.3 μm completely absorbed by ozone in the upper atmosphere.
Photographic UV band	0.3 to 0.4 μm	Transmitted through the atmosphere. Detectable with film and photodetectors, but atmospheric scattering is severe.
Visible region	0.4 to 0.7 μm	Imaged with film and photodetectors. Includes reflected energy peak of earth at 0.5 μm.
Infrared region	0.7 to 1000 μm	Interaction with matter varies with wavelength. Atmospheric transmission windows are separated by absorption bands.
Reflected IR band	0.7 to 3.0 μm	Reflected solar radiation that contains no information about thermal properties of materials. The interval from 0.7 to 0.9 μm is detectable with film and is called the photographic IR band.
Thermal IR band	3 to 5 μm, 8 to 14 μm	Principal atmospheric windows in the thermal region. Images at these wavelengths are acquired by optical-mechanical scanners and special vidicon systems but not by film.
Microwave region	0.1 to 100 cm	Longer wavelengths that can penetrate clouds, fog, and rain. Images may be acquired in the active or passive mode.
Radar	0.1 to 100 cm	Active form of microwave remote sensing. Radar images are acquired at various wavelength bands.
Radio	>100 cm	Longest-wavelength portion of electromagnetic spectrum.

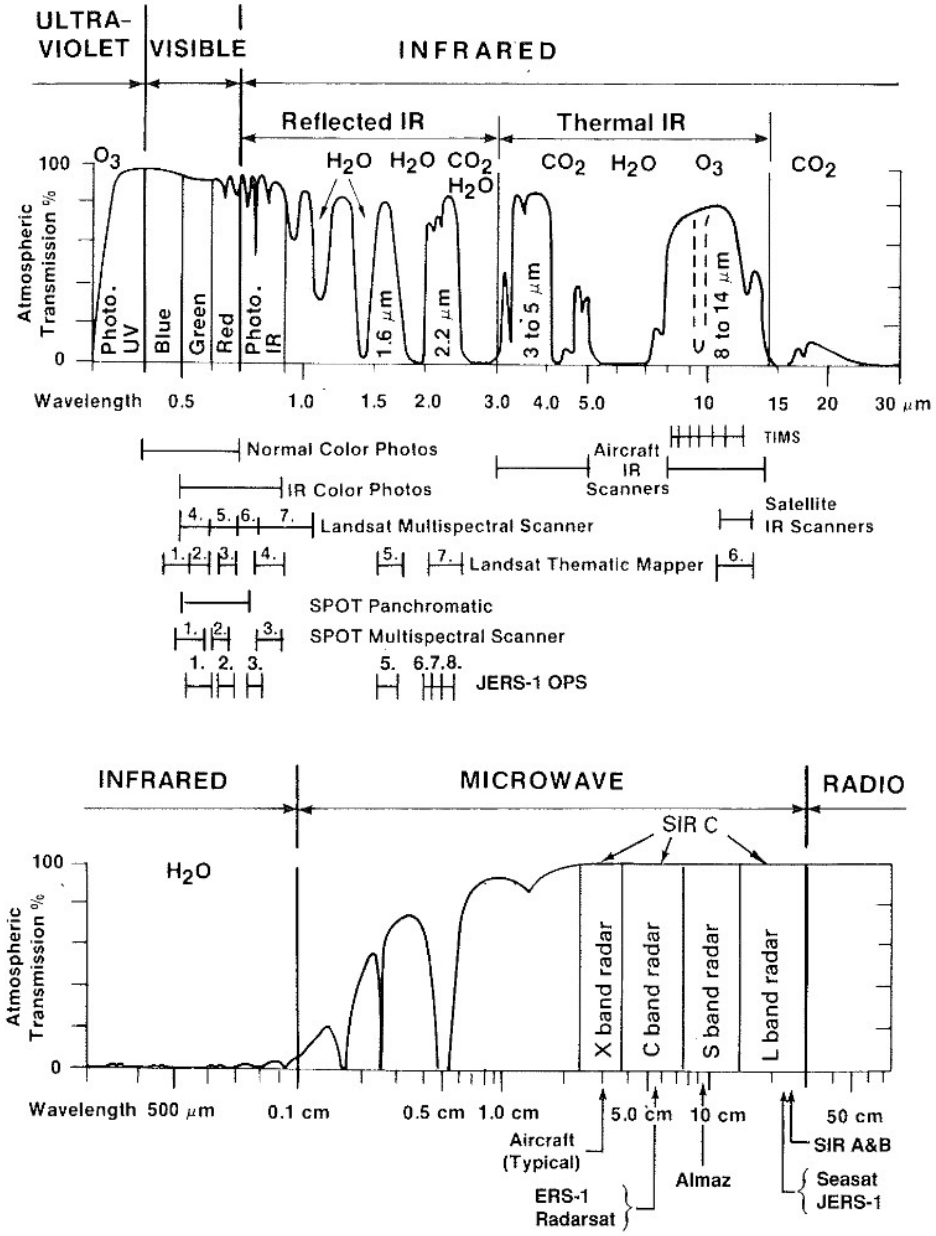

Figure 1-3 Expanded diagrams of the visible and infrared regions (upper) and microwave regions (lower) for transmission through the atmosphere. Gases responsible for atmospheric absorption bands are indicated. Wavelength bands recorded by commonly used remote sensing systems are shown (middle).

earth during daytime may be recorded as a function of wavelength. The maximum amount of energy is reflected at the 0.5-μm wavelength, which corresponds to the green wavelengths of the visible region and is called the *reflected energy peak* (Figure 1-2). The earth also radiates energy both day and night, with the maximum energy radiating at the 9.7-μm wavelength. This *radiant energy peak* occurs in the thermal portion of the IR region (Figure 1-2).

The earth's atmosphere absorbs energy in the gamma-ray, X-ray, and most of the ultraviolet (UV) regions; therefore, these regions are not used for remote sensing. Terrestrial remote sensing records energy in the microwave, infrared, and visible regions, as well as the long wavelength portion of the UV region. Figure 1-3 shows details of these regions. The horizontal axes show wavelength on a logarithmic scale; the vertical axes show the percentage of electromagnetic energy that is transmitted

through the earth's atmosphere. Wavelength intervals with high transmission are called *atmospheric windows* and are used to acquire remote sensing images. The major remote sensing regions (visible, infrared, and microwave) are further subdivided into *bands*, such as the blue, green, and red bands of the visible region (Figure 1-3). Horizontal lines in the center of the diagram show wavelength bands in the UV through thermal IR regions recorded by major imaging systems such as cameras and scanners. For the Landsat systems, the numbers identify specific bands recorded by these systems. The characteristics of the remote sensing regions are summarized in Table 1-3.

Passive remote sensing systems record the energy that naturally radiates or reflects from an object. An *active* system supplies its own source of energy, directing it at the object in order to measure the returned energy. Flash photography is an example of active remote sensing, in contrast to available light photography, which is passive. Another common form of active remote sensing is radar (Table 1-3), which provides its own source of electromagnetic energy at microwave wavelengths. Sonar systems transmit pulses of sonic energy.

Atmospheric Effects

Our eyes inform us that the atmosphere is essentially transparent to light, and we tend to assume that this condition exists for all electromagnetic energy. In fact, the gases of the atmosphere absorb electromagnetic energy at specific wavelength intervals called *absorption bands*. Figure 1-3 shows these absorption bands together with the gases in the atmosphere responsible for the absorption.

Wavelengths shorter than 0.3 μm are completely absorbed by the ozone (O_3) layer in the upper atmosphere (Figure 1-3). This absorption is essential to life on earth, because prolonged exposure to the intense energy of these short wavelengths destroys living tissue. For example, sunburn occurs more readily at high mountain elevations than at sea level. Sunburn is caused by UV energy, much of which is absorbed by the atmosphere at sea level. At higher elevations, however, there is less atmosphere to absorb the UV energy.

Clouds consist of aerosol-sized particles of liquid water that absorb and scatter electromagnetic radiation at wavelengths less than about 0.1 cm. Only radiation of microwave and longer wavelengths is capable of penetrating clouds without being scattered, reflected, or absorbed.

IMAGE CHARACTERISTICS

In general usage, an *image* is any pictorial representation, irrespective of the wavelength or imaging device used to produce it. A *photograph* is a type of image that records wavelengths from 0.3 to 0.9 μm that have interacted with light-sensitive chemicals in photographic film. Images can be described in terms of certain fundamental properties regardless of the wavelength at which the image is recorded. These properties are scale, brightness, contrast, and resolution. The tone and texture of images are functions of the fundamental properties.

Scale

Scale is the ratio of the distance between two points on an image to the corresponding distance on the ground. A common scale on U.S. Geological Survey topographic maps is 1:24,000, which means that one unit on the map equals 24,000 units on the ground. Thus 1 cm on the map represents 24,000 cm (240 m) on the ground, or 1 in. represents 24,000 in. (2000 ft). The maps and images of this book show scales graphically as bars.

The deployment of imaging systems on satellites has changed the concepts of image scale. In this book, scales of images are designated as follows:

Small scale (greater than 1:500,000)	1 cm = 5 km or more (1 in. = 8 mi or more)
Intermediate scale (1:50,000 to 1:500,000)	1 cm = 0.5 to 5 km) (1 in. = 0.8 to 8 mi)
Large scale (less than 1:50,000)	1 cm = 0.5 km or less (1 in. = 0.8 mi or less)

These designations differ from the traditional scale concepts of aerial photography. Forty years ago, 1:62,500 was the minimum scale of commercially available photographs and was considered small-scale. Today sensing systems on high-altitude aircraft and satellites can acquire photographs and images of excellent quality at much smaller scales. Optimum image scale is determined by how the images are to be interpreted. With the advent of satellite images, many investigators have been surprised at the amount and types of information that can be interpreted from very small scale images.

Brightness and Tone

Remote sensing systems detect the intensity of electromagnetic radiation that an object reflects, emits, or scatters at particular wavelength bands. Variations in intensity of electromagnetic radiation from the terrain are displayed as variations in brightness on images. On positive images, such as those in this book, the brightness of objects is directly proportional to the intensity of electromagnetic radiation that is detected from that object.

Brightness is the magnitude of the response produced in the eye by light; it is a subjective sensation that can be determined only approximately. *Luminance* is a quantitative measure of the intensity of light from a source and is measured with a device called a photometer, or light meter. People who interpret images rarely, if ever, make quantitative measurements of brightness variations on an image. Variations in brightness may be calibrated with a gray scale such as the one in Figure 1-4. Each distinguishable shade from black to white is a separate *tone*. In practice, most interpreters do not use an actual gray scale the way one would use a centimeter scale; they character-

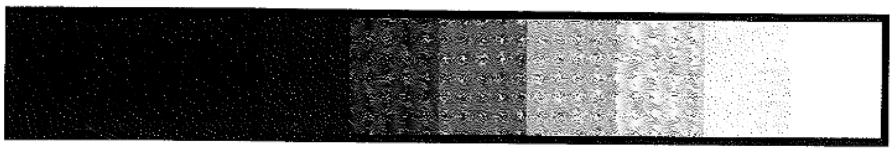

Figure 1-4 Gray scale.

ize areas on an image as light, intermediate, or dark in tone using their own mental concept of a gray scale.

On aerial photographs the tone of an object is primarily determined by the ability of the object to reflect incident sunlight, although atmospheric effects and the spectral sensitivity of the film are also factors. On images acquired at other wavelength regions, tone is determined by other physical properties of objects. On thermal IR images the tone of an object is proportional to the heat radiating from the object. On radar images the tone of an object is determined by the intensity at which the transmitted beam of radar energy is scattered back to the receiving antenna.

Contrast Ratio

Contrast ratio (*CR*) is the ratio between the brightest and darkest parts of the image and is defined as

$$CR = \frac{B_{max}}{B_{min}} \tag{1-3}$$

where B_{max} is the maximum brightness of the scene and B_{min} is the minimum brightness. Figure 1-5 shows images of high, medium, and low contrast, together with profiles of brightness variation across each image. On a brightness scale of 0 to 10, these images have the following contrast ratios:

A. High contrast $CR = \frac{9}{2} = 4.5$

B. Medium contrast $CR = \frac{5}{2} = 2.5$

C. Low contrast $CR = \frac{3}{2} = 1.5$

Note that when $B_{min} = 0$, CR is infinity; when $B_{min} = B_{max}$, CR is unity. This discussion is summarized from the extensive review by Slater (1983), which describes other terms for contrast. In addition to describing an entire scene, contrast ratio is

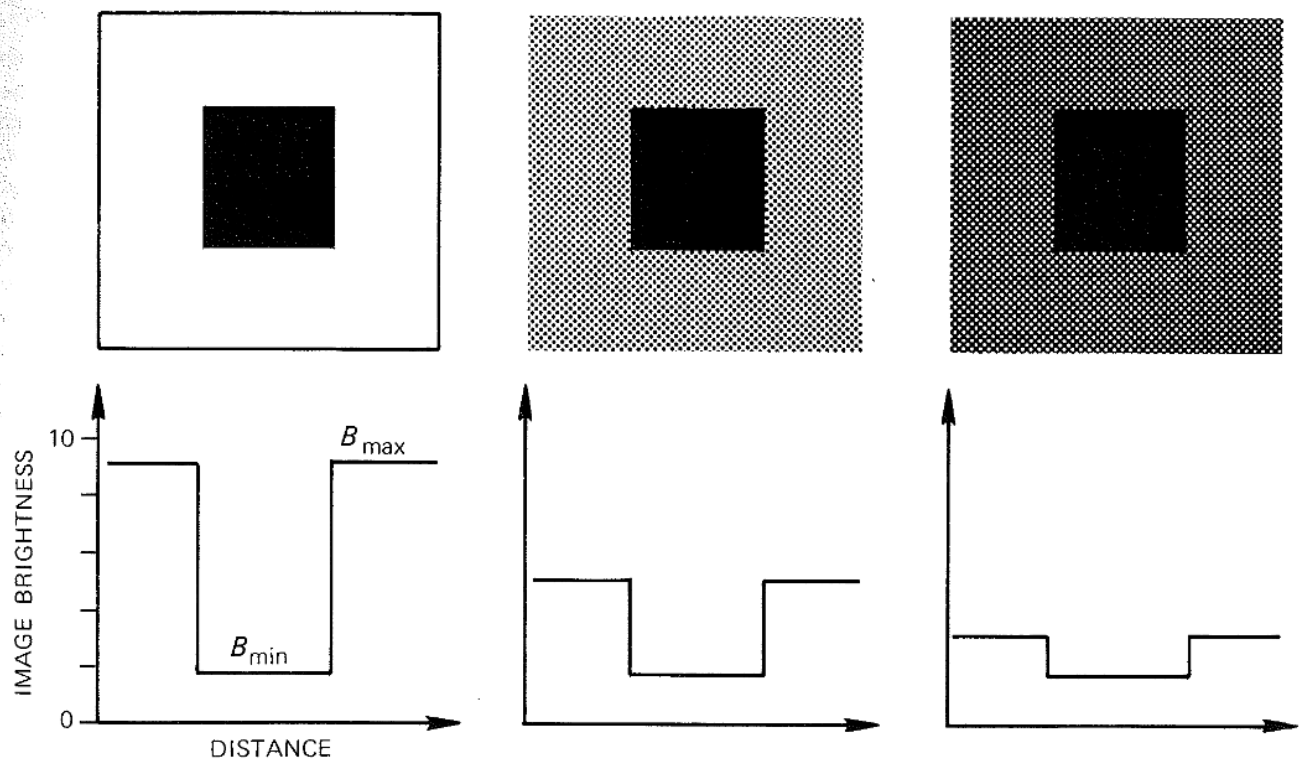

A. High contrast ratio. B. Medium contrast ratio. C. Low contrast ratio.

Figure 1-5 Images of different contrast ratios (upper) with corresponding brightness profiles (lower).

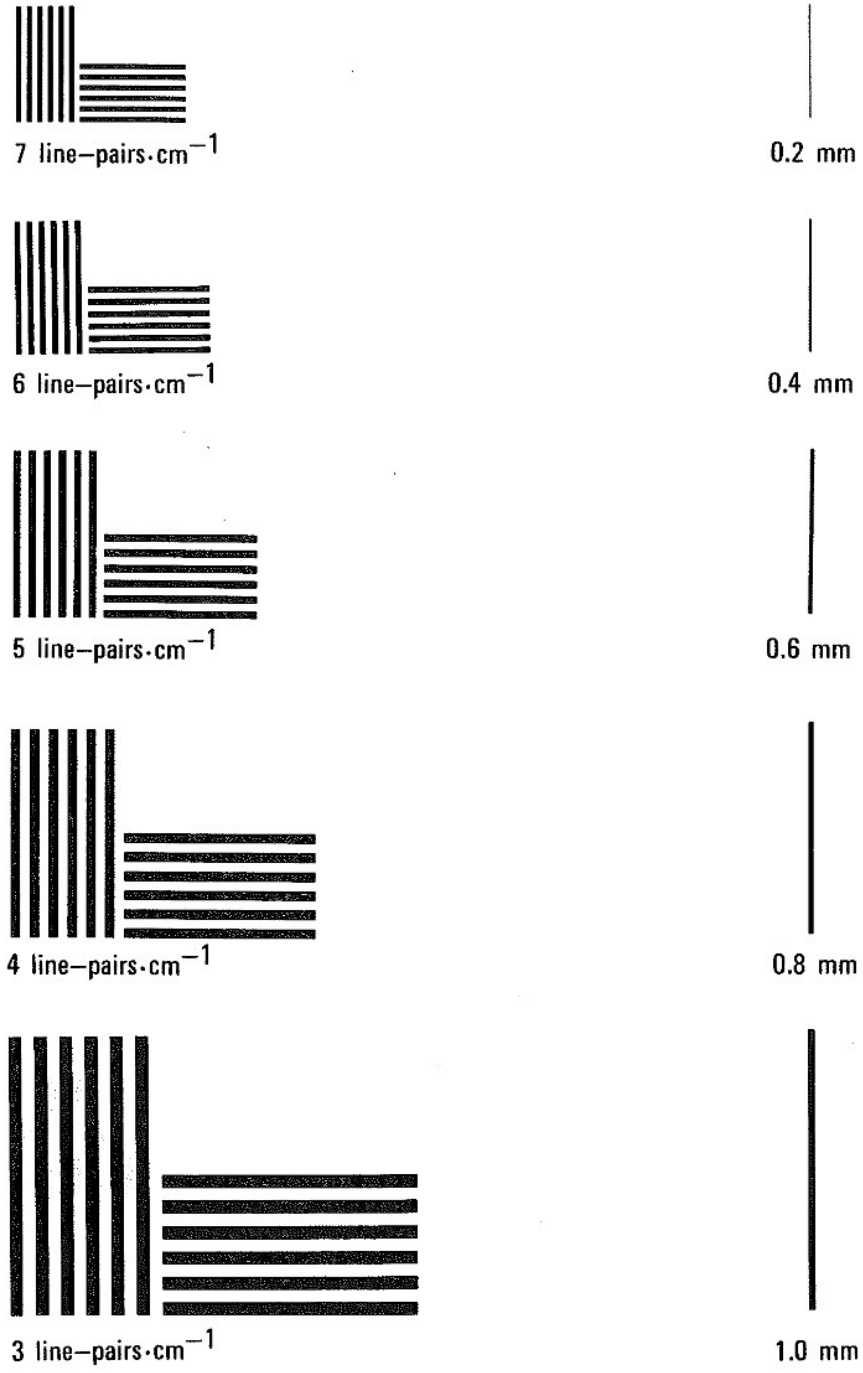

Figure 1-6 Resolution and detection targets with high contrast ratio. View this chart from a distance of 5 m (16.5 ft). For A, determine the most closely spaced set of bars you can resolve. For B, determine the narrowest line you can detect.

also used to describe the ratio between the brightness of an object on an image and the brightness of the adjacent background. Contrast ratio is a vital factor in determining the ability to resolve and detect objects.

Images with a low contrast ratio are commonly referred to as "washed out," with monotonous, nearly uniform tones of gray. Low contrast may result from the following causes:

1. The objects and background of the scene may have a nearly uniform electromagnetic response at the particular wavelength band that the remote sensing system recorded. In other words, the scene has an inherently low contrast ratio.
2. Scattering of electromagnetic energy by the atmosphere can reduce the contrast of a scene. This effect is most pronounced in the shorter-wavelength portions of the photographic remote sensing band, as described in Chapter 2.
3. The remote sensing system may lack sufficient sensitivity to detect and record the contrast of the terrain. Incorrect recording techniques can also result in low contrast images even though the scene has a high contrast ratio when recorded by other means.

A low contrast ratio, regardless of the cause, can be improved by digital enhancement methods, as described in Chapter 8.

Spatial Resolution and Resolving Power

This book defines *spatial resolution* as the ability to distinguish between two closely spaced objects on an image. More specifically, it is the minimum distance between two objects at which the images of the objects appear distinct and separate. Objects spaced together more closely than the resolution limit will appear as a single object on the image. Forshaw and others (1983) discuss alternative definitions of spatial resolution.

Resolving power and spatial resolution are two closely related concepts. The term *resolving power* applies to an imaging system or a component of the system, whereas *spatial resolution* applies to the image produced by the system. For example, the lens and film of a camera system each have a characteristic resolving power that, together with other factors, determines the resolution of the photographs.

Spatial resolution of a photographic system is customarily determined by photographing a standard resolution target, such as the one shown in Figure 1-6A, under specified conditions of illumination and magnification. The resolution targets, or *bar charts*, consist of alternating black and white bars of equal width called *line-pairs*. Spacing of resolution targets is expressed in line-pairs. For the target with 5 line-pairs · cm^{-1}, each black bar is 0.1 cm wide and separated by a white bar of the same width. The photograph is viewed under magnification, and the observer determines the most closely spaced set of line-pairs for which the bars and spaces are discernible. Spatial resolution of the photographic system is stated as the number of line-pairs per millimeter of the resolved target.

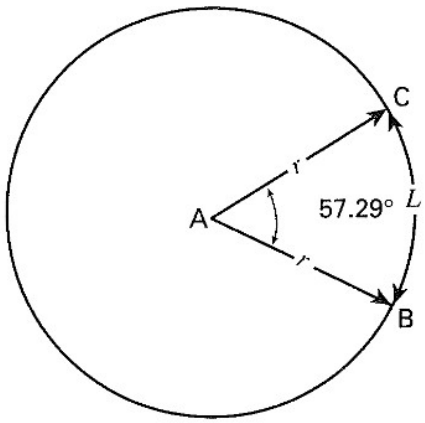

Figure 1-7 Radian system of angular measurement.

Human judgment and visual characteristics are critical components in this analysis, which therefore is not completely objective and reproducible. Spatial resolution is different for objects of different shape, size, arrangement, and contrast ratio. An alternative method of describing resolution is the *modulation transfer function* (MTF), which employs a bar chart with progressively closer spacing of the bars (McKinney, 1980).

An alternative method of measuring spatial resolution is *angular resolving power*, which is defined as the angle subtended by imaginary lines passing from the imaging system and two targets spaced at the minimum resolvable distance. Angular resolving power is commonly measured in radians. As shown in Figure 1-7, a *radian* (rad) is the angle subtended by an arc BC of a circle having a length equal to the radius AB of the circle. Because the circumference of a circle has a length equal to 2π times the radius, there are 2π, or 6.28, rad in a circle. A radian corresponds to 57.3° or 3438 min, and one milliradian (mrad) is 10^{-3} rad. In the radian system of angular measurement,

$$\text{Angle} = \frac{L}{r} \text{ rad} \tag{1-4}$$

where L is the length of the subtended arc and r is the radius of the circle. A convenient relationship is that at a distance r of 1000 units, 1 mrad subtends an arc L of 1 unit. Figure 1-8 illustrates the angular resolving power of a remote sensing system (the eye) that can resolve the center bar chart of Figure 1-6 at a distance of 5 m. This chart has 5 line-pairs · cm^{-1}, and the bars are separated by 1 mm. For these targets with a high contrast ratio, the angular resolving power is 0.2 mrad.

Resolving power and spatial resolution will be discussed for each remote sensing system described in this book, but you should remember the following points:

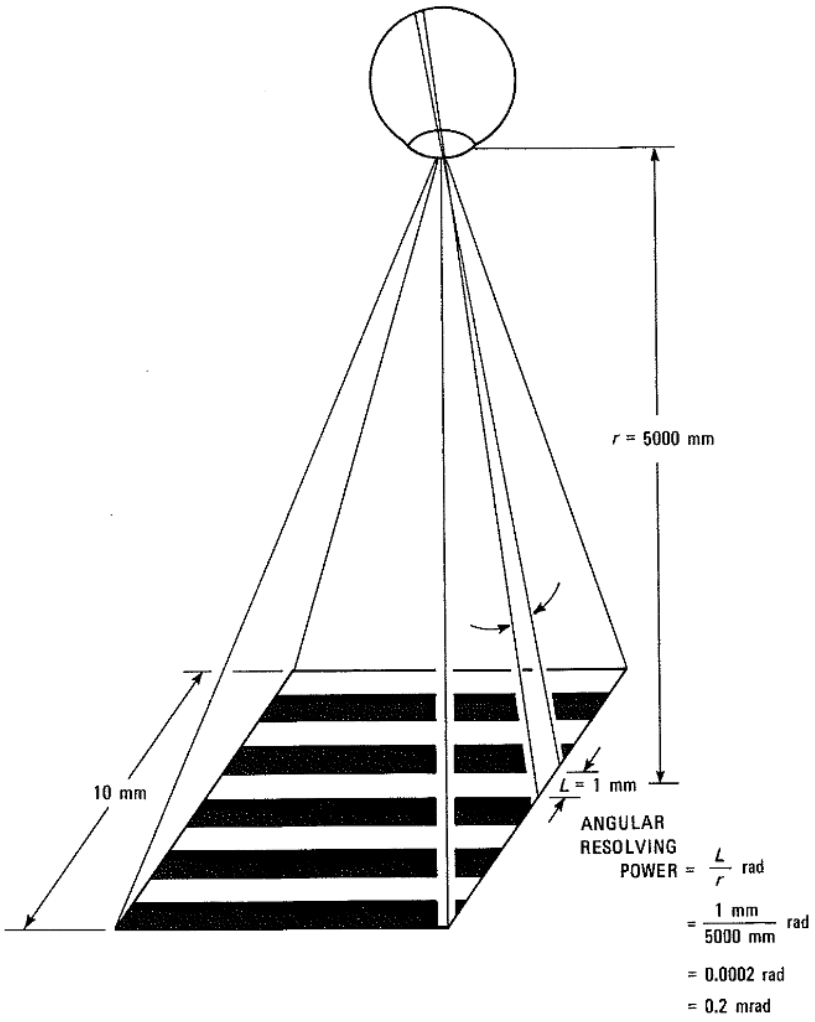

Figure 1-8 Angular resolving power (in milliradians) for a remote sensing system that can resolve 5 line-pairs • cm^{-1} at a distance of 5 m.

1. Theoretical resolving power of a system is rarely achieved in actual operation.
2. Resolution alone does not adequately determine whether an image is suitable for a particular application.
3. Resolution is the minimum separation between two objects for which the images appear distinct and separate; it is *not* the size of the smallest object that can be seen. By knowing the resolution and scale of an image, however, one can estimate the size of the smallest detectable object.

Other Characteristics of Images

Detectability is the ability of an imaging system to record the presence or absence of an object, although the identity of the object may be unknown. An object may be detected even though it is smaller than the theoretical resolving power of the imaging system.

Recognizability is the ability to identify an object on an image. Objects may be detected and resolved and yet not be recognizable. For example, roads on an image appear as narrow lines that could also be railroads or canals. Unlike resolution, there are no quantitative measures for recognizability and detectability. It is important for the interpreter to understand the significance and correct use of these terms. Rosenberg (1971) summarizes the distinctions between them.

A *signature* is the expression of an object on an image that enables the object to be recognized. Characteristics of an object that control its interaction with electromagnetic energy determine its signature. For example, the spectral signature of an object is its brightness measured at a specific wavelength of energy.

Texture is the frequency of change and arrangement of tones on an image. *Fine, medium,* and *coarse* are qualitative terms used to describe texture.

An *interpretation key* is a characteristic or combination of characteristics that enables an object to be identified on an image. Typical keys are size, shape, tone, and color. The associations of different characteristics are valuable keys. On images of cities, one may recognize single-family residential areas by the association of a dense street network, lawns, and small buildings. The associations of certain landforms and vegetation species are keys for identifying different types of rocks.

VISION

Of our five senses, two (touch and vision) detect electromagnetic radiation. Some of the nerve endings in our skin detect thermal IR radiation as heat but do not form images. Vision is the most important sense and accounts for most of the information input to our brain. Vision is not only an important remote sensing system in its own right, but it is also the means by which we interpret the images produced by other remote sensing systems. The following section analyzes the human eye as a remote sensing system. Much of the information is summarized from Gregory (1966).

Structure of the Eye

For such a complex structure, the human eye (Figure 1-9) appears deceptively simple. Light enters through the clear *cornea*, which is separated from the lens by fluid called the *aqueous humor*. The *iris* is the pigmented part of the eye that controls the variable aperture called the *pupil*. It is commonly thought that variations in pupil size allow the eye to function over a wide range of light intensities. However, the pupil varies in area over a ratio of only 16:1 (that is, the maximum area is 16 times the minimum area), whereas the eye functions over a brightness range of about 100,000:1. The pupil contracts to limit the light rays to the central and optically best part of the lens, except when the full opening is needed in dim light. The pupil also contracts for near vision, increasing the depth of field for near objects.

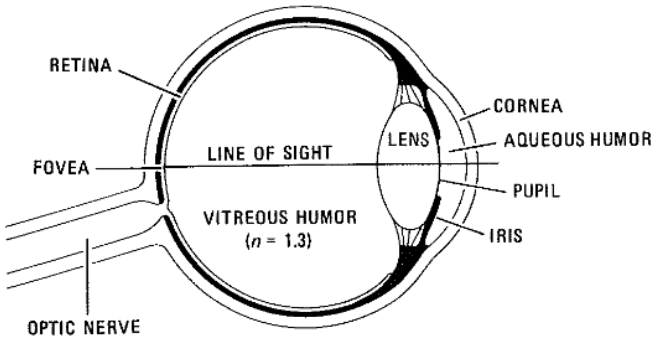

Figure 1-9 Structure of the human eye.

A common misconception is that the lens *refracts* (bends) the incoming rays of light to form the image. The amount that light bends when passing through two adjacent media is determined by the difference in the refractive indices (n) of the two media; the greater the difference, the greater the bending. For the eye, the maximum difference is between air (n = 1.0) and the cornea (n = 1.3), and this interface is where the maximum light refraction occurs. Although the lens is relatively unimportant for forming the image, it is important in *accommodating*, or focusing, for near and far vision. In cameras, this accommodation is done by changing the position of the lens relative to the film. In the human eye, the shape rather than the position of the lens is changed by muscles that vary the tension on the lens. For near-vision tension, the muscles release, allowing the lens to become thicker in the center and assume a more convex cross section. With age, the cells of the lens harden and the lens becomes too rigid to accommodate for different distances; this is the time in life when bifocal glasses may become necessary to provide for near and far vision.

An inverted image is focused on the *retina*, a thin sheet of interconnected nerve cells that includes the light receptor cells called rods and cones, which convert light into electrical impulses. The rods and cones receive their names from their longitudinal shapes when viewed microscopically. The cones function in daylight conditions to give color, or *photopic*, vision. The rods function under low illumination and give vision only in tones of gray, called *scotopic* vision. Rods and cones are not uniformly distributed throughout the retinal surface. The maximum concentration and organization of receptor cells is in the *fovea* (Figure 1-9), a small region at the center of the retina that provides maximum visual acuity. You can demonstrate the existence and importance of the fovea by concentrating on a single letter on this page. The rest of the page and even the nearby words and letters will appear indistinct because they are outside the field of view of the fovea. The eye is in continual motion to bring the fovea to bear on all parts of the page or scene. Close to the fovea is the blind spot, where the optic nerve joins the eye and there are no receptor cells. The electrical impulses from the receptor cells are transmitted to the brain, which interprets them as visual perception.

Resolving Power of the Eye

The diameter of the largest receptor cells in the fovea (3 μm) determines the resolving power of the eye. Multiplying this diameter maximum by the refractive index of the vitreous humor (n = 1.3) determines an effective diameter (4 μm) for the receptor cells. The *image distance*, or distance from the retina to the lens, is about 20 mm, or 20,000 μm. The effective width of the receptors is 4/20,000 (1/5000) of the image distance. Image distance is proportional to *object distance*, which is the distance from the eye to the object. An object forms an image that

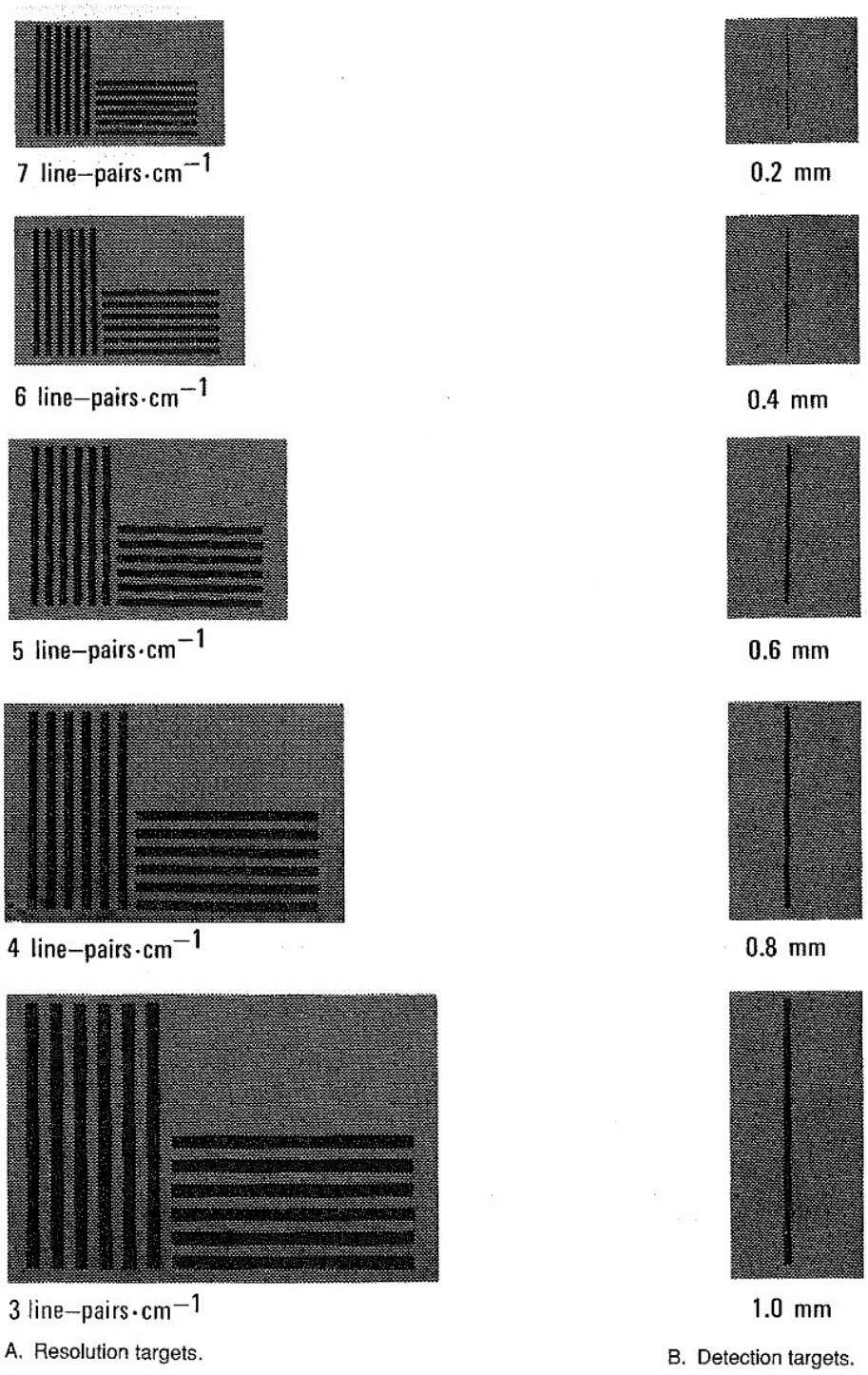

Figure 1-10
Resolution and detection targets with medium contrast ratio. View this chart from a distance of 5 m (16.5 ft). For A, determine the most closely spaced set of bars you can resolve. For B, determine the narrowest line you can detect. Compare these values with those determined for Figure 1-6.

fills the width of a receptor if the object width is 1/5000 the object distance. Therefore, adjacent objects must be separated by 1/5000 the object distance for their images to fall on alternate receptors and be resolved by the eye.

You can estimate the resolving power of your eyes in the following manner. View the resolution targets of Figure 1-6A at a distance of 5 m (16.4 ft), and determine the most closely spaced set of line-pairs that you can resolve. Also determine the narrowest of the bars in Figure 1-6B that you can detect. Make these determinations now, before reading further, because the following text may influence your perception of the targets.

For the high-contrast resolution targets of Figure 1-6A at a distance of 5 m, the normal eye should be able to resolve the middle set that has 5 line-pairs · cm^{-1}. The black and white bars are 1 mm wide. The *instantaneous field of view* (*IFOV*) of any detector is the solid angle through which a detector is sensitive to radiation. Equation 1-4 is used to calculate the *IFOV* of the eye, where the radius (r) is 5000 mm and the length of the subtended arc (L) is 1 mm:

$$IFOV = \frac{L}{r} \text{ rad} \quad (1\text{-}4)$$

$$= \frac{1 \text{ mm}}{5000 \text{ mm}} \text{ rad}$$

$$= 0.2 \times 10^{-3} \text{ rad}$$

$$= 0.2 \text{ mrad}$$

Figure 1-8 shows the relationships of the resolution targets to the *IFOV* of the eye. The 0.2-mrad *IFOV* of the eye means that at a distance of 1000 units, the eye can resolve high-contrast targets that are spaced no closer than 0.2 units.

Detection Capability of the Eye

When the detection targets of Figure 1-6B are viewed from a distance of 5 m, most readers can detect the narrowest bar, which is 0.2 mm wide. Recall, however, that at this distance the minimum separation at which bar targets can be resolved is 1.0 mm. This test illustrates the difference between resolution and detection.

Detection is influenced not only by the size of objects but also by their shape and orientation. For example, if dots are used in place of lines in Figure 1-6B, the diameter of the smallest detectable dot would be considerably larger than 0.2 mm.

Effect of Contrast Ratio on Resolution and Detection

The resolution and detection targets in Figure 1-10 have the same spacing as those in Figure 1-6, but the contrast ratio has been reduced by the addition of a gray background. To evaluate the effect of the lower contrast ratio, view Figure 1-10 from a distance of 5 m, and determine which targets can be resolved and detected. Using this figure, most readers can resolve only 3 line-pairs · cm^{-1}, and the smallest detectable target is the 0.6-mm-wide line. These dimensions are larger than the 5 line-pairs · cm^{-1} and the 0.2-mm line of the high-contrast target and demonstrate the effect of a lower contrast ratio on resolution and detection.

REMOTE SENSING SYSTEMS

The eye is a familiar example of a remote sensing system. The inorganic remote sensing systems described in this book belong to the two major categories: framing systems and scanning systems.

Framing Systems

Framing systems instantaneously acquire an image of an area, or *frame*, on the terrain. Cameras and vidicons are common examples of such systems (Figure 1-11). A *camera* employs a

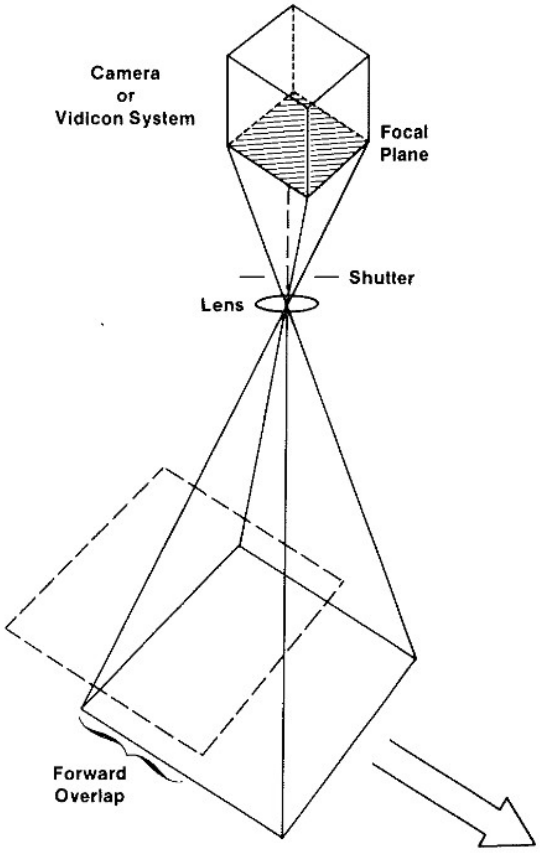

Figure 1-11 Framing system for acquiring remote sensing images. Cameras and vidicons are framing systems.

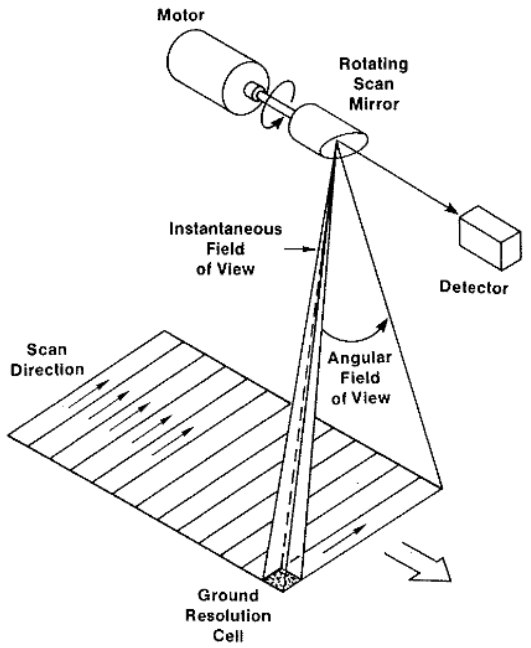

A. Cross-track scanner.

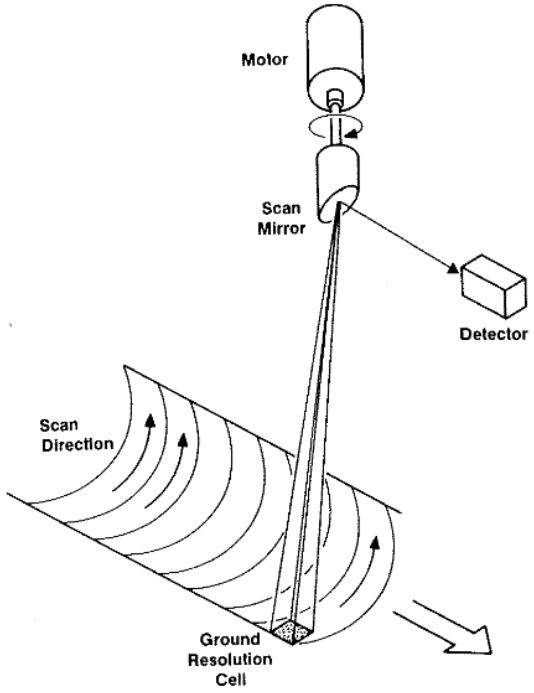

B. Circular scanner.

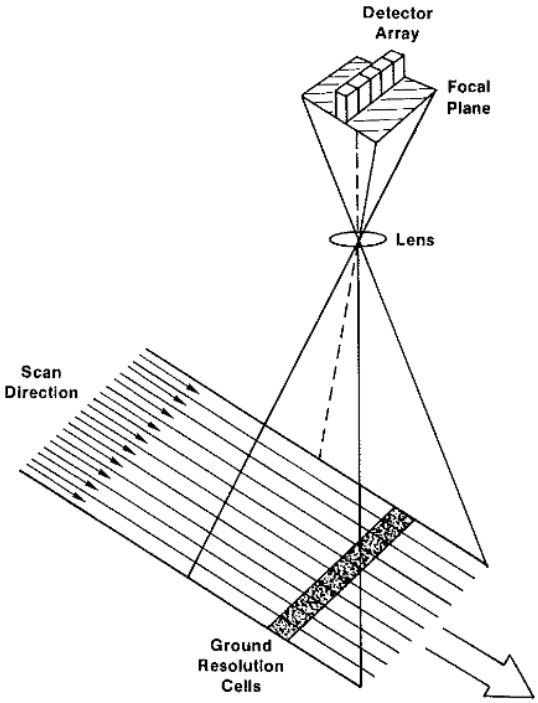

C. Along-track scanner.

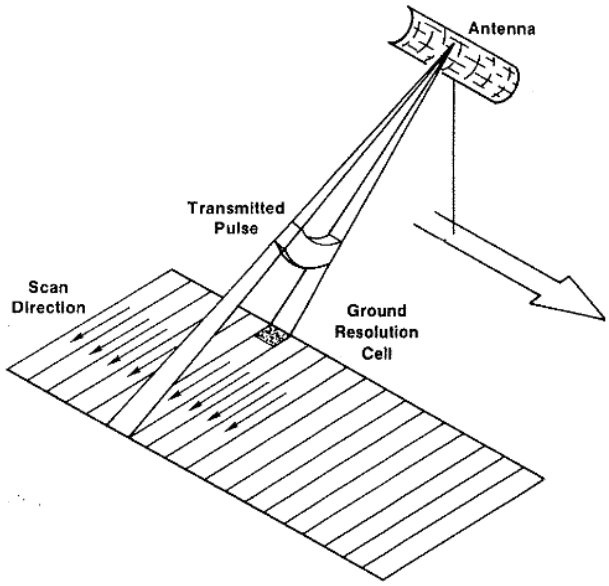

D. Side-scanning system.

Figure 1-12 Scanning systems for acquiring remote sensing images.

lens to form an image of the scene at the *focal plane,* which is the plane at which the image is sharply defined. A shutter opens at selected intervals to allow light to enter the camera, where the image is recorded on photographic film. A *vidicon* is a type of television camera that records the image on a photosensitive electronically charged surface. An electron beam then sweeps the surface to detect the pattern of charge differences that constitute the image. The electron beam produces a signal that may be transmitted and recorded on magnetic tape for eventual display on film.

Successive frames of camera and vidicon images may be acquired with *forward overlap* (Figure 1-11). The overlapping portions of the two frames may be viewed with a stereoscope to produce a three-dimensional view, as described in Chapter 2. Film is sensitive only to portions of the UV, visible, and reflected IR regions (0.3 to 0.9 μm). Special vidicons are sensitive into the thermal band of the IR region. A framing system can instantaneously image a large area because the system has a dense array of detectors located at the focal plane: The retina of the eye has a network of rods and cones, the emulsion of camera film contains tiny grains of silver halide, and a vidicon surface is coated with sensitive phosphors.

Scanning Systems

A *scanning system* employs a single detector with a narrow field of view that is swept across the terrain to produce an image. When photons of electromagnetic energy radiated or reflected from the terrain encounter the detector, an electrical signal is produced that varies in proportion to the number of photons. The electrical signal is amplified, recorded on magnetic tape, and played back later to produce an image. All scanning systems sweep the detector's field of view across the terrain in a series of parallel scan lines. Figure 1-12 shows the four common scanning modes: cross-track scanning, circular scanning, along-track scanning, and side scanning.

Cross-Track Scanners The widely used *cross-track scanners* employ a faceted mirror that is rotated by an electric motor, with a horizontal axis of rotation aligned parallel with the flight direction (Figure 1-12A). The mirror sweeps across the terrain in a pattern of parallel scan lines oriented *normal* (perpendicular) to the flight direction. Energy radiated or reflected from the ground is focused onto the detector by secondary mirrors (not shown). Images recorded by cross-track scanners, and other scanner systems, are described by two characteristics: spectral resolution and spatial resolution.

Spectral resolution refers to the wavelength interval that is recorded by a detector. In Figure 1-13 the vertical scale shows the response, or signal strength, of a detector as a function of wavelength, shown in the horizontal scale. As the wavelength increases, the detector response increases to a maximum and then decreases. Spectral resolution, or *bandwidth,* is defined as the wavelength interval recorded at 50 percent of the peak

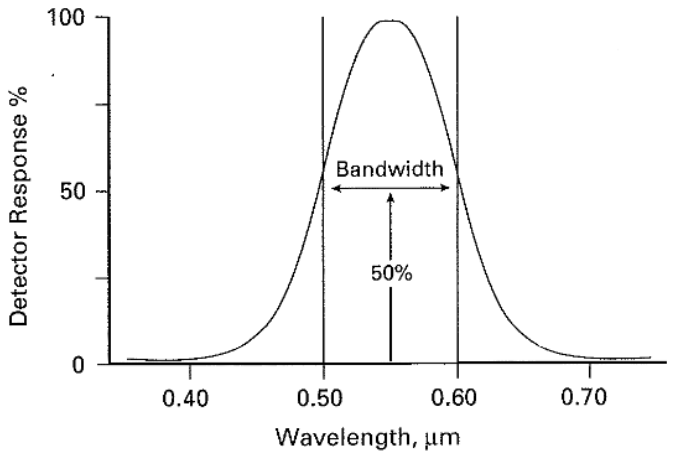

Figure 1-13 Spectral resolution, or bandwidth, of a detector. Bandwidth of this detector is 0.10 μm.

response of a detector. In Figure 1-13 the 50 percent limits occur at 0.50 and 0.60 μm, corresponding to a bandwidth of 10 μm. The section on Reflectance Spectra from Hyperspectral Data describes the effects of different bandwidths on image data.

Spatial resolution was defined earlier, using the eye as an example. The physical dimensions of a detector determine its spatial resolution which is expressed as angular resolving power, measured in milliradians (mrad). Angular resolving power determines the *IFOV* (defined earlier). As shown in Figure 1-12A, the *IFOV* subtends an area on the terrain called a *ground resolution cell.* Dimensions of a ground resolution cell are determined by the detector IFOV and the altitude of the scanning system. A detector with an *IFOV* of 1 mrad at an altitude of 10 km subtends a ground resolution cell of 10 by 10 m. Figure 1-14 shows the important relationship between size of ground resolution cells and spatial resolution of images. The different cell sizes for Figure 1-14B–D were produced by computer processing of the original 10-m data of Figure 1-14A. The images cover a portion of the town of Victorville, California, and the adjacent desert terrain (Figure 1-15). Resolving fine spatial detail of the urban area requires 10-by-10-m cells. Larger linear features, such as the fault and the Mojave River are detectable with 30-by-30-m cells. The images in Figure 1-14 are shown at a large scale (1:24,000), where the 10-m version is obviously optimum. At smaller scales (1:100,00), however, larger cells, such as 30 m (Figure 1-14C), produce readily interpretable images.

The *angular field of view* (Figure 1-12A) is that portion of the mirror sweep, measured in degrees, that is recorded as a scan line. The angular field of view and the altitude of the system determine the *ground swath,* which is the width of the

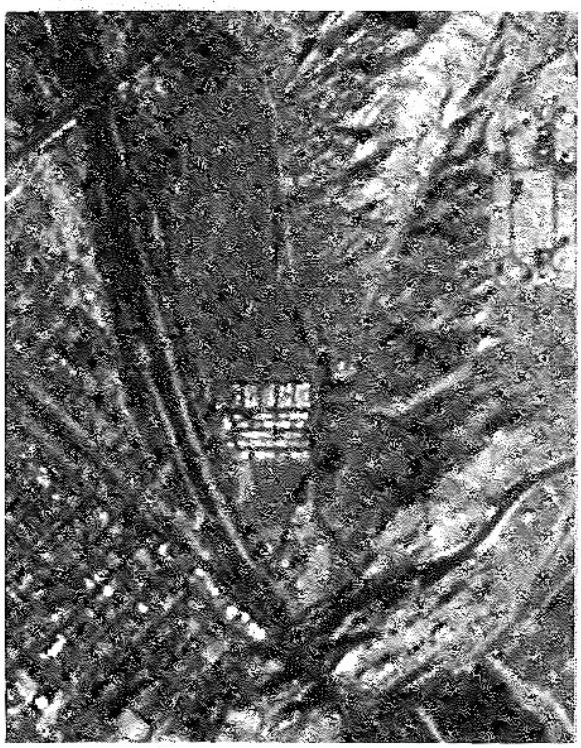

A. 10 by 10 m.

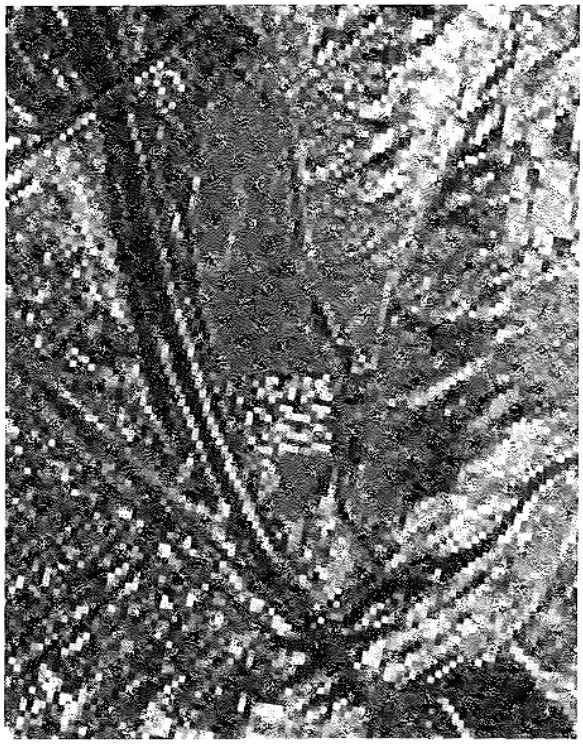

B. 20 by 20 m.

C. 30 by 30 m.

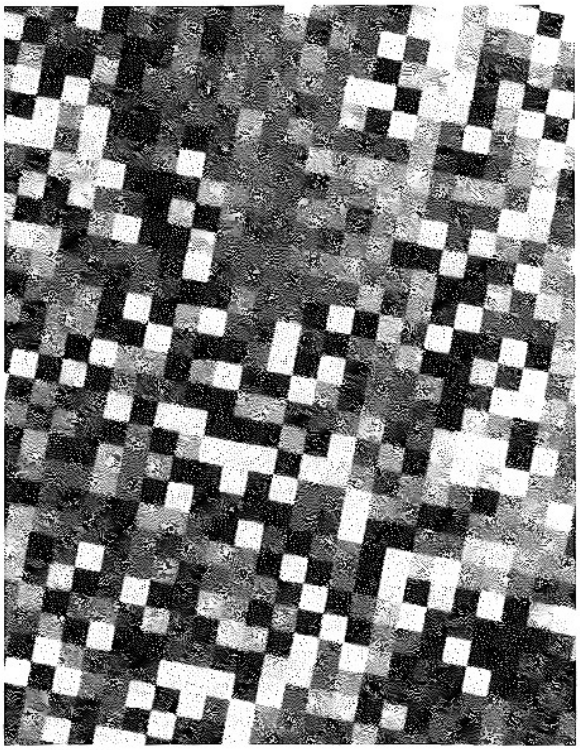

D. 80 by 80 m.

Figure 1-14 Images displayed with different ground resolution cells. Spatial resolution is determined by the size of the cell. The area is a portion of Victorville in southern California.

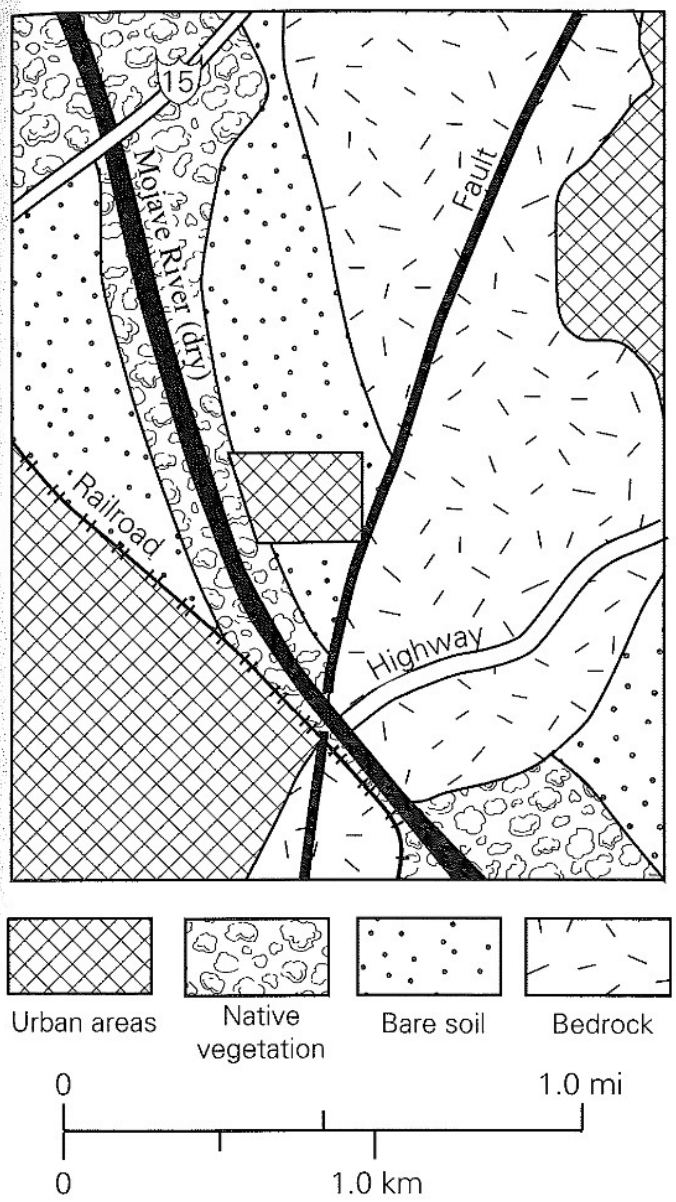

Figure 1-15 Location map of Victorville, California, showing land-cover categories.

terrain strip represented by the image. Ground swath is calculated as

$$\text{Ground swath} = \tan\left(\frac{\text{angular field of view}}{2}\right) \times \text{altitude} \times 2 \qquad (1\text{-}6)$$

The distance between the scanner and terrain is greater at the margins of the ground swath than at the center of the swath. As a result, ground resolution cells are larger toward the margins than at the center, which results in a geometric distortion that is characteristic of cross-track scanner images. This distortion is corrected by digital processing, as shown in Chapter 8.

At the high altitude of satellites, a narrow angular field of view is sufficient to cover a broad swath of terrain. For this reason the rotating mirror is replaced by a flat mirror that oscillates back and forth through an angle of approximately 15°. An example is the scanner of Landsat described in Chapter 3.

The strength of the signal generated by a detector is a function of the following factors:

Energy flux The amount of energy reflected or radiated from terrain is the *energy flux*. For visible detectors, this flux is lower on a dark day than on a sunny day.

Altitude For a given ground resolution cell, the amount of energy reaching the detector is inversely proportional to the square of the distance. At greater altitudes the signal strength is weaker.

Spectral bandwidth of the detector The signal is stronger for detectors that respond to a broader bandwidth of energy. For example, a detector that is sensitive to the entire visible range will receive more energy than a detector that is sensitive to a narrow band, such as visible red.

Instantaneous field of view Both the physical size of the sensitive element of the detector and the effective focal length of the scanner optics determine the *IFOV*. A small *IFOV* is required for high spatial resolution but also restricts the *signal strength* (amount of energy received by the detector).

Dwell time The time required for the detector *IFOV* to sweep across a ground resolution cell is the *dwell time*. A longer dwell time allows more energy to impinge on the detector, which creates a stronger signal.

For a cross-track scanner, the dwell time is determined by the detector *IFOV* and by the velocity at which the scan mirror sweeps the *IFOV* across the terrain. As shown in Figure 1-16A a typical airborne scanner with a detector *IFOV* of 1 mrad, a 90° angular field of view, and operating at 2×10^{-2} sec per scan line at an altitude of 10 km has a dwell time of 1×10^{-5} sec per ground resolution cell. It is instructive to compare the dwell time with the ground speed of the aircraft. At a typical ground speed of 720 km · h^{-1}, or 200 m · sec^{-1}, the aircraft crosses the 10 m of a ground resolution cell in 5×10^{-2} sec. The cross-track scanner time of 1×10^{-5} is 5×10^{3} times faster than the ground velocity of the aircraft. The high scanner speed relative to ground speed is required to prevent gaps between adjacent scan lines.

The short dwell time of cross-track scanners imposes constraints on the other factors that determine signal strength. For example, the *IFOV* and spectral bandwidth must be large enough to produce a signal of sufficient strength to overcome the inherent electronic noise of the system. The signal-to-noise ratio must be sufficiently high for the signal to be recognizable.

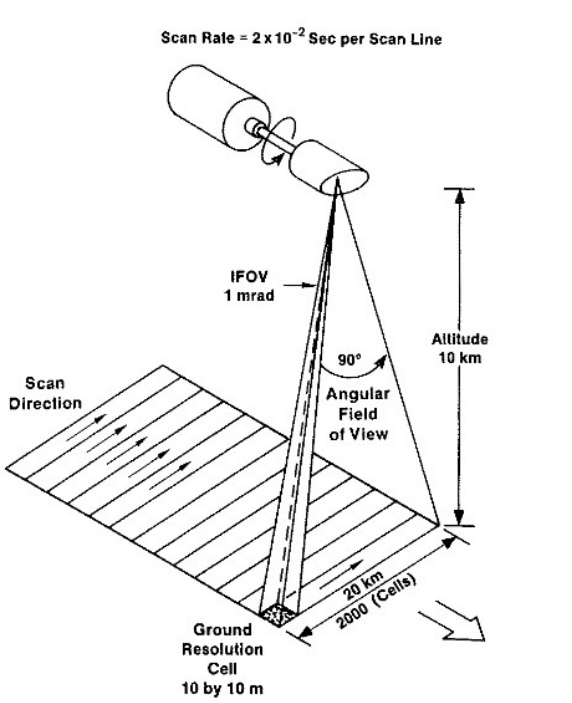

$$\text{Dwell Time} = \frac{\text{Scan Rate per Line}}{\text{Number Cells per Line}} = \frac{2 \times 10^{-2}\ \text{sec}}{2000\ \text{cells}} = 1 \times 10^{-5}\ \text{sec} \cdot \text{cell}^{-1}$$

A. Cross-track scanner.

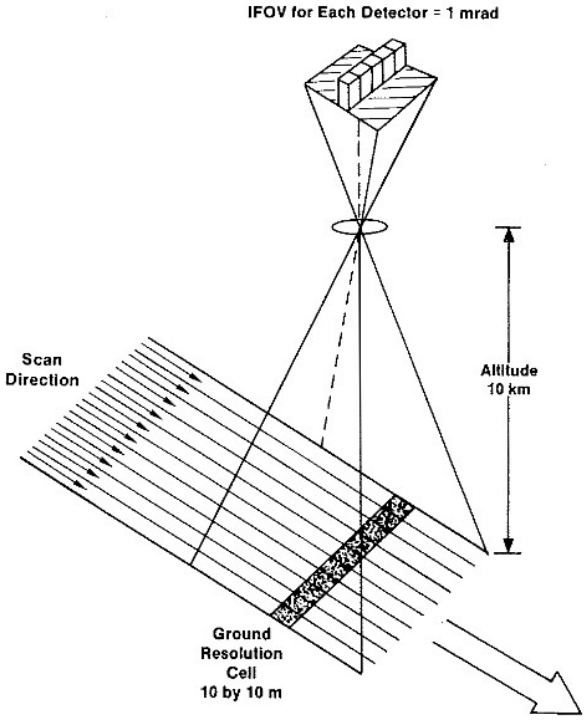

$$\text{Dwell Time} = \frac{\text{Cell Dimension}}{\text{Velocity}} = \frac{10\ \text{m} \cdot \text{cell}^{-1}}{200\ \text{m} \cdot \text{sec}^{-1}} = 5 \times 10^{-2}\ \text{sec} \cdot \text{cell}^{-1}$$

B. Along-track scanner.

Figure 1-16 Dwell time calculated for cross-track and along-track scanners.

Circular Scanners In a *circular scanner* the scan motor and mirror are mounted with a vertical axis of rotation that sweeps a circular path on the terrain (Figure 1-12B). Only the forward portion of the sweep is recorded to produce images. An advantage of this system is that the distance between scanner and terrain is constant and all the ground resolution cells have the same dimensions. The major disadvantage is that most image processing and display systems are designed for linear scan data; therefore the circular scan data must be extensively reformatted prior to processing.

Circular scanners are used for reconnaissance purposes in aircraft. The axis of rotation is tilted forward to acquire images of the terrain well in advance of the aircraft position. The images are displayed in real time on a screen in the cockpit to guide the pilot. Airborne circular scanners with IR detectors are called FLIR (forward looking IR) systems.

Along-Track Scanners For scanner systems to achieve finer spatial and spectral resolution, the dwell time for each ground resolution cell must be increased. One method is to eliminate the scanning mirror and provide an individual detector for each ground resolution cell across the ground swath (Figure 1-12C). The detectors are placed in a linear array in the focal plane of the image formed by a lens system.

The long axis of the linear array is oriented normal to the flight path, and the *IFOV* of each detector sweeps a ground resolution cell along the terrain parallel with the flight track direction (Figure 1-12C). *Along-track scanning* refers to this movement of the ground resolution cells. These systems are also called pushbroom scanners because the detectors are analogous to the bristles of a broom pushed along the floor.

For along-track scanners, the dwell time of a ground resolution cell is determined solely by the ground velocity, as Figure 1-16B illustrates. For a jet aircraft flying at 720 km · h^{-1}, or 200 m · sec^{-1}, the along-track dwell time for a 10-m cell is 5×10^{-2} sec, which is 5×10^{3} times greater than the dwell time for a comparable cross-track scanner. The increased dwell time allows two improvements: (1) detectors can have a smaller *IFOV*, which provides finer spatial resolution, and (2) detectors can have a narrower spectral bandwidth, which provides higher spectral resolution. Some experimental airborne along-track scanners operate with a spectral bandwidth of 0.01 μm. Typical cross-track scanners have bandwidths of 0.10 μm, which is a spectral resolution coarser by one order of magnitude.

Side-Scanning Systems The cross-track, circular, and along-track scanners just described are passive systems, since they detect and record energy naturally reflected or radiated from the terrain. Active systems, which provide their own energy sources, operate primarily in the *side-scanning mode*. The example in Figure 1-12D is a radar system that transmits pulses of microwave energy to one side of the flight path (range direction) and records the energy scattered from the terrain back to the antenna, as described in Chapter 6. Another system is side-scanning sonar, which transmits pulses of sonic energy in the ocean to map bathymetric features (Chapter 9).

Scanner Systems Compared Cross-track and along-track scanners have different characteristics that are summarized in the following chart.

	Cross-track scanner	*Along-track scanner*
Angular field of view	Wider	Narrower
Mechanical system	Complex	Simple
Optical system	Simple	Complex
Spectral range of detectors	Wider range	Narrower range, but expanding
Dwell time	Shorter	Longer

The selection of a scanner system involves a number of choices, or trade-offs. Cross-track scanners are generally preferred for reconnaissance surveys because the wider angular field of view records images with a wide swath width. Along-track scanners are preferred for recording detailed spectral and spatial information. The longer dwell time can accommodate detectors with a narrow bandwidth or a small *IFOV*.

SPECTRAL REFLECTANCE CURVES

The various framing and scanning systems record images. Another important aspect of remote sensing is the acquisition of nonimaging data. *Spectral reflectance curves,* or reflectance spectra, record the percentage of incident energy, typically sunlight, that is reflected by a material as a function of wavelength of the energy. Figure 1-17 shows reflectance spectra of vegetation and typical rocks. The horizontal axis shows the wavelength of incident energy, which ranges from the visible into reflected IR spectral regions. The vertical axis shows the percentage of incident energy reflected at the different wavelengths. The curves are offset vertically to prevent confusing overlaps. Downward excursions of a curve are called *absorption features* because they represent absorption of incident energy. Upward excursions are called *reflectance peaks*. These spectral features are valuable clues for recognizing materials, such as the rocks in Figure 1-17, on remote sensing images. For this reason reflectance spectra of many materials have

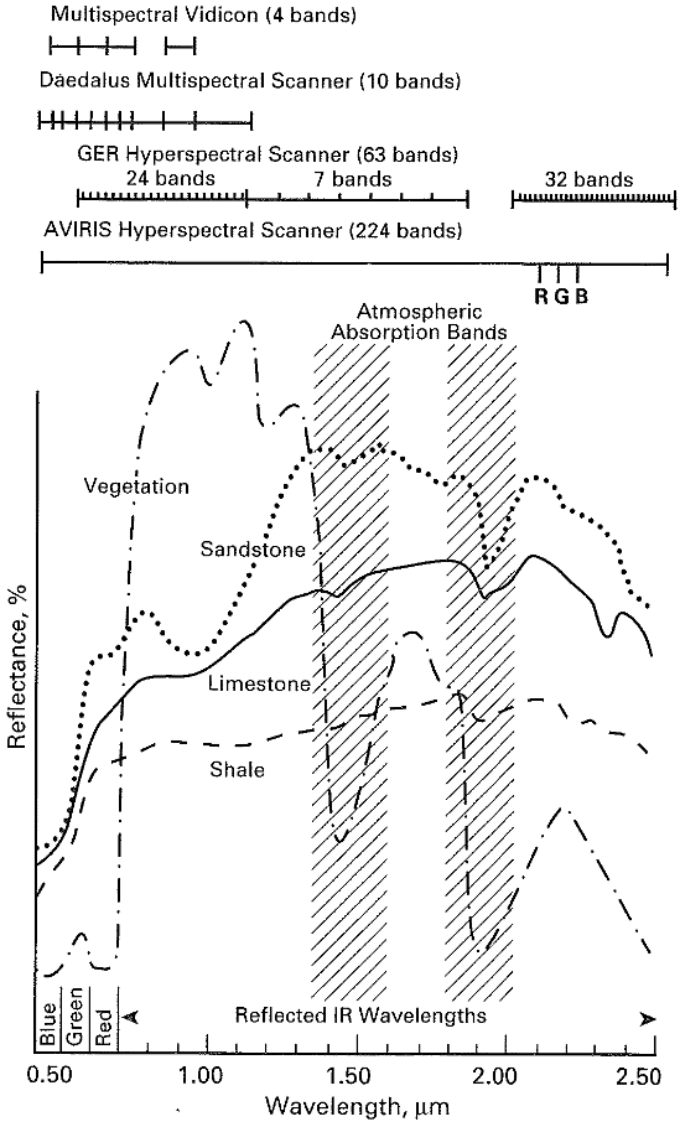

Figure 1-17 Reflectance spectra of rocks and vegetation. Spectral bands of typical multispectral and hyperspectral systems are shown.

been recorded and published. Hunt (1980) published a number of mineral spectra and explained the interactions between energy and matter that cause the spectral features at different wavelengths. Hunt (1980) also provided references to his extensive publications of spectra of rocks and minerals. Clark and others (1990) described laboratory spectroscopy and the causes of absorption features in mineral spectra. They also provide an extensive collection of mineral spectra. Grove and others (1992) published laboratory spectra of 150 minerals. Price (1995) describes 11 published collections of reflectance spectra in the visible and reflected IR regions (0.4 to 2.5 μm) that include soils, agriculture, grasses, shrubs, rocks, minerals, fabrics, metals, and building materials. Price assembled the 3417

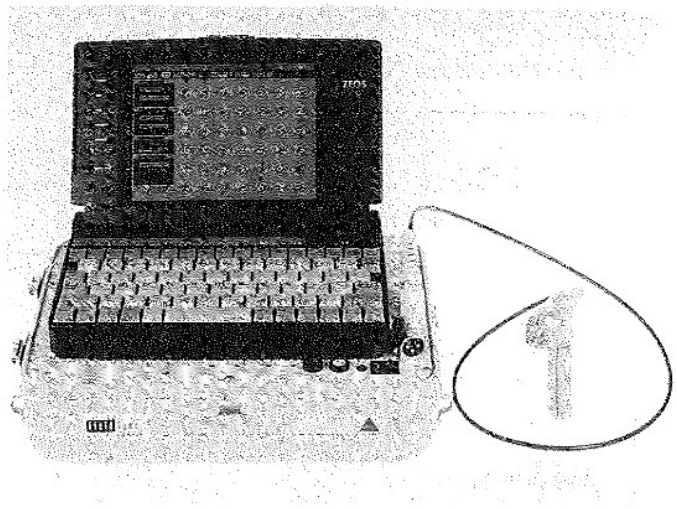

Figure 1-18 Spectrometer for recording reflectance spectra in the field or laboratory. Courtesy Analytical Spectral Devices, Inc., Boulder, CO.

spectra into a standardized digital format on a personal computer diskette. Copies of the diskette are available for research purposes from

J. C. Price
Beltsville Agricultural Research Center
USDA Agricultural Research Service
Beltsville, MD 20705

These spectra should be useful for comparing and identifying spectra recorded from hyperspectral scanners, which are described in a following section.

Reflectance spectra are recorded by instruments called *reflectance spectrometers*. Figure 1-18 is a typical spectrometer that may be used in the field. In the laboratory it uses a light source that matches the characteristics of sunlight. Modern spectrometers record spectra in a digital format that may be displayed directly in real time on the screen of a laptop computer. Some spectrometer systems provide a digital reference library of spectra of known materials, such as rocks, soils, and vegetation. Optional software can compare the spectrum of an unknown material with the library and provide a possible identification. This spectral matching technique is subject to misidentifications, however, as analyzed by Price (1994).

Some manufacturers of spectrometers suitable for remote sensing are listed below; readers may contact them for information on specifications, optional equipment, and cost.

Analytical Spectral Devices (ASD)
4760 Walnut Street, Suite 105
Boulder, CO 80301
Phone: 303-444-6522

Geophysical & Environmental Research Corp. (GER)
One Bennett Common
Millbrook, NY 12545
Phone 914-677-6100

Integrated Spectronics Pty. Ltd.
P.O. Box 437
Baulkham Hill
NSW, 2153, Australia
Phone: 02-887-8760

The ground resolution cell of a handheld spectrometer covers only a few square centimeters. The ground resolution cell of a scanner in an aircraft or satellite covers tens to hundreds of square meters. Because of this difference in coverage one must be cautious when using spectra to evaluate scanner images. Longshaw (1976) analyzed and described the problems of using laboratory spectra to interpret images of rock outcrops.

MULTISPECTRAL IMAGING SYSTEMS

A *multispectral image* is an array of simultaneously acquired images that record separate wavelength intervals, or bands. Multispectral images differ from images such as conventional photographs, which record a single image that spans a broad spectral range. Much of this book deals with multispectral images that are acquired in all the remote sensing spectral regions. Slater (1985) provides a survey of multispectral systems.

Multispectral systems differ in the following characteristics:

- Imaging technology—framing or scanning method
- Total spectral range recorded
- Number of spectral bands recorded
- Range of wavelengths recorded by each spectral band (bandwidth)

The upper portion of Figure 1-17 shows the wavelength bands recorded by representative aircraft multispectral systems, which are listed in Table 1-4 and described in the following sections. Multispectral systems are also widely used in satellites, as described in subsequent chapters. Multispectral images are acquired by two methods: framing systems or scanning systems.

Multispectral Framing Systems

The simplest multispectral framing systems consist of several cameras or vidicons mounted together and aligned to acquire simultaneous multiple images of an area. Today the preponderance of multispectral imagery is acquired by scanners, but vidicon framing systems serve a useful purpose.

Multispectral Cameras *Multispectral cameras* employ a range of film and filter combinations to acquire black-and-

Table 1-4 Representative aircraft multispectral imaging systems

System	*Technology*	*Spectral range, μm*	*Bands*	*Bandwidth, μm*
Vidicon	Framing (vidicon)	0.40 to 0.90	4	0.10
Daedalus scanner	Scanning (cross-track)	0.38 to 1.10	10	0.03 to 0.20
GER scanner	Scanning (cross-track)	0.50 to 2.50	63	0.025 to 0.175
AVIRIS scanner	Scanning (cross-track)	0.40 to 2.50	224	0.010
SFSI scanner	Scanning (along-track)	1.22 to 2.42	115	0.010

white photographs that record narrow spectral bands. The shutters are linked together and triggered simultaneously. These systems are also called *multiband cameras*. These were the original multispectral systems and are mentioned for historical purposes because they have essentially been replaced by vidicon systems. Lowman (1969) and the National Aeronautics and Space Administration (NASA, 1977) show examples of multispectral photographs.

Multispectral Vidicons *Multispectral vidicons* operate in two modes: (1) two or more individual systems record images at different wavelength bands, or (2) a single system records multiple bands. Several multispectral vidicon systems have been configured; these range from two to four black-and-white vidicons that record narrow bands in the visible and reflected IR regions. Marsh and others (1991) used a two-vidicon system that records red and reflected IR bands to analyze a hazardous waste site in Arizona. The system was also used to assess land cover in the Mato Grosso, Brazil (Marsh, Walsh, and Sobrevila, 1994). Neale and Crowther (1994) assembled a system from three commercial vidicons that records green, red, and reflected IR bands.

Table 1-4 lists the characteristics of a commercial aircraft vidicon system that acquires four spectral bands (blue, green, red, and reflected IR) that can be composited into color images. Monday and others (1994) used such images to map the city of Irving, Texas (70 mi^2), in 8 months, rather than the 3 years estimated for conventional mapping. King (1995) describes the technology and applications of multispectral vidicon systems and provides references to related publications.

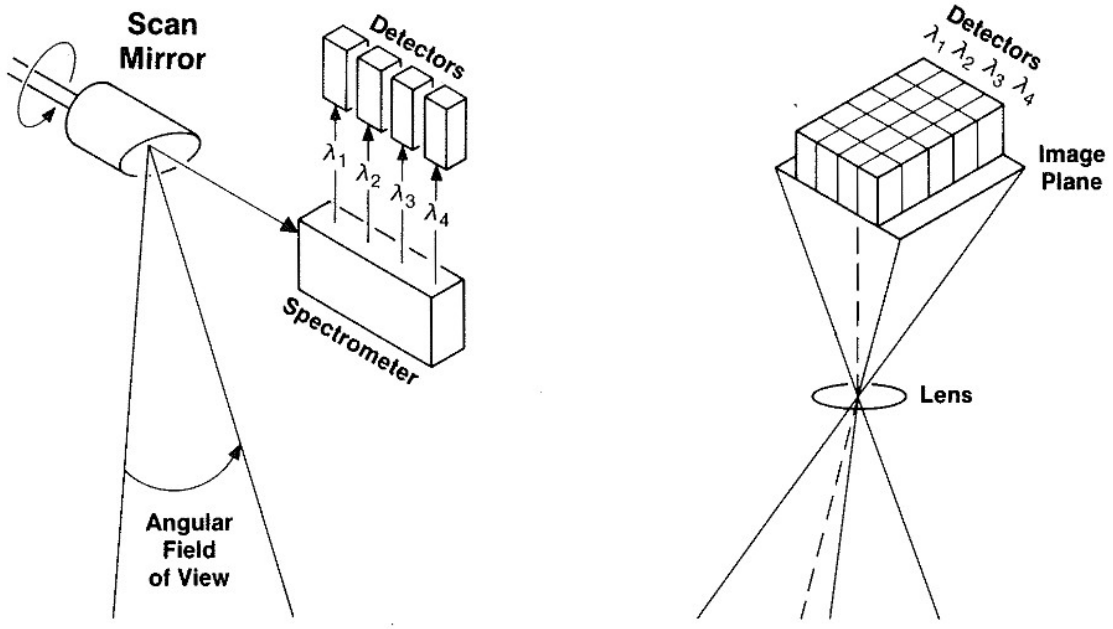

A. Cross-track. B. Along-track.

Figure 1-19 Multispectral scanner systems.

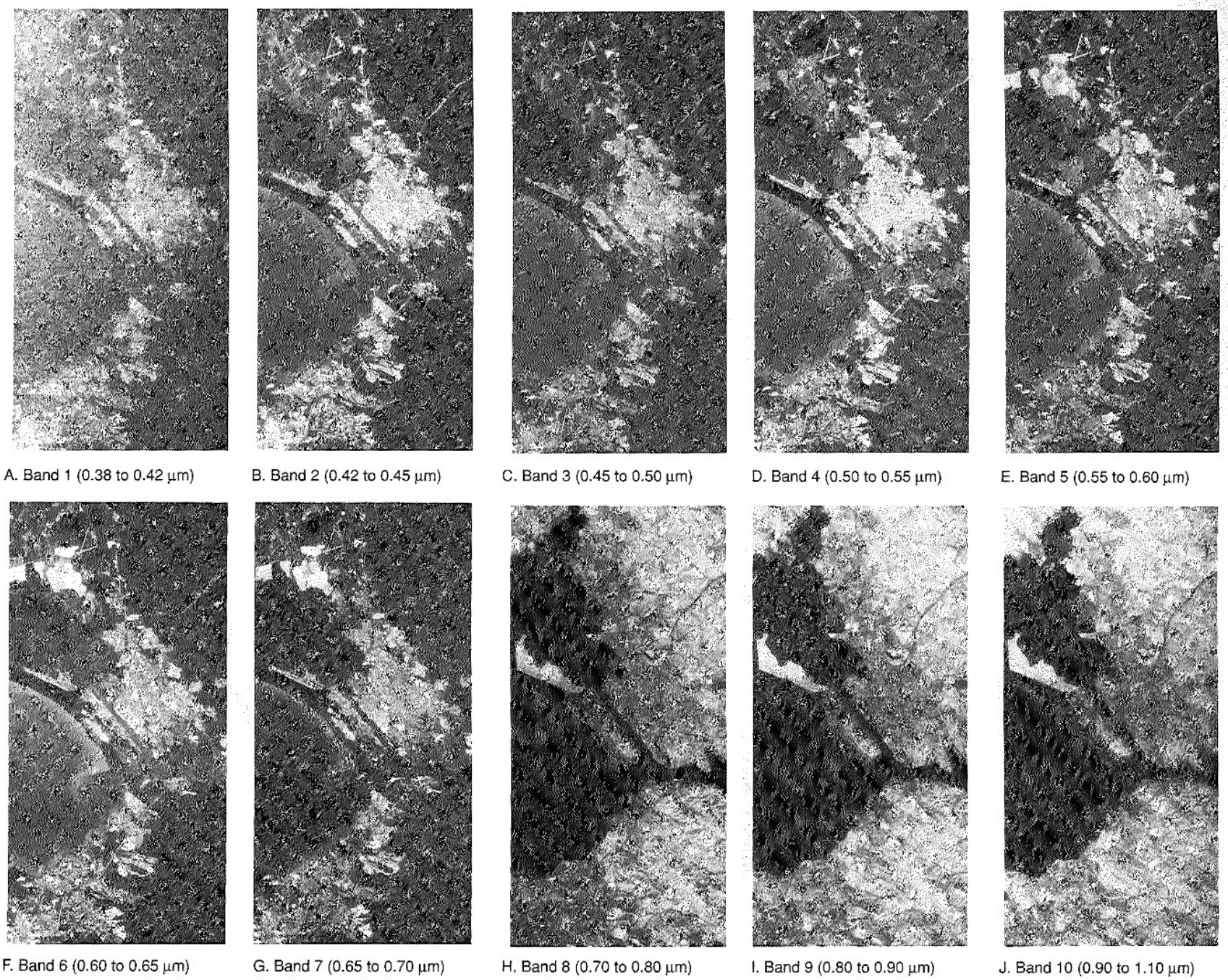

A. Band 1 (0.38 to 0.42 μm) B. Band 2 (0.42 to 0.45 μm) C. Band 3 (0.45 to 0.50 μm) D. Band 4 (0.50 to 0.55 μm) E. Band 5 (0.55 to 0.60 μm)

F. Band 6 (0.60 to 0.65 μm) G. Band 7 (0.65 to 0.70 μm) H. Band 8 (0.70 to 0.80 μm) I. Band 9 (0.80 to 0.90 μm) J. Band 10 (0.90 to 1.10 μm)

Figure 1-20 Aircraft multispectral scanner images of San Pablo Bay, California, acquired March 28, 1980. Each image covers an area of 15 by 30 km. Courtesy NASA Ames Research Center.

Multispectral Scanning Systems

Multispectral scanner systems are widely used to acquire images from aircraft and satellites. Both cross-track and along-track systems are used.

Cross-Track Multispectral Scanner Images Cross-track scanners employ a spectrometer to disperse the incoming energy into a spectrum (Figure 1-19A). Detectors are positioned to record specific wavelength bands of energy (denoted $\lambda_1 \cdots \lambda_4$ in the figure). Figure 1-20 shows images of San Pablo Bay, California, acquired by a cross-track multispectral scanner manufactured by the Daedalus Corporation. Figure 1-21 shows the categories of land use and land cover in the San Pablo Bay area, which is the northern extension of San Francisco Bay. Table 1-5 lists the characteristics of the scanner and the 10 multispectral images. Plate 1A is a color composite image that was prepared by projecting bands 2 (blue), 4 (green), and 7 (red) in blue, green, and red, respectively. Many other color combinations can easily be created.

The black-and-white images of the individual spectral bands (Figure 1-20) demonstrate the relationships among wavelength, atmospheric scattering, contrast ratio, and spatial resolution. Band 1 in the UV and blue region records the shortest wavelengths of all the bands and has the maximum atmospheric scattering, resulting in a low contrast ratio and poor spatial resolution. The network of streets in the city of Vallejo is a useful resolution target; as the wavelength of the images increases, the ability to discern the streets improves and reaches a maximum in the reflected IR region (bands 8, 9, and 10).

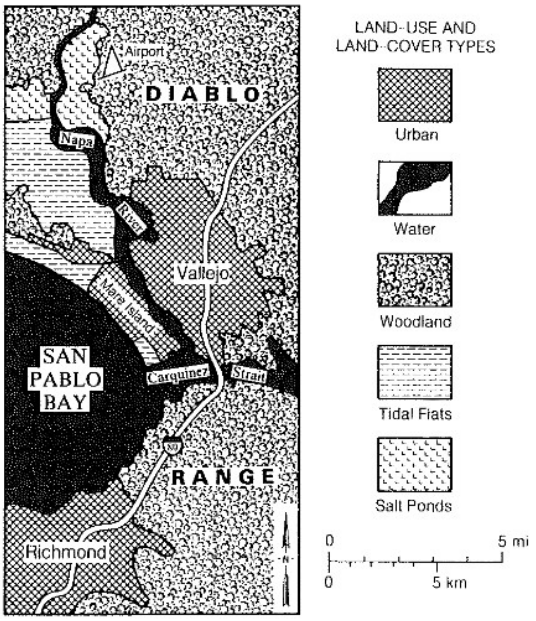

Figure 1-21 Land-use and land-cover types of the San Pablo Bay area, California, interpreted from aircraft multispectral scanner images.

TABLE 1-5 Daedalus aircraft multispectral scanner and images

Aircraft altitude	19.5 km
Scanner *IFOV*	1.25 mrad
Ground resolution cell	24 by 24 m
Scan angle	42°
Image swath width	14.7 km

*Band**	*Wavelength, μm*	*Spectral band*
1	0.38 to 0.42	UV and blue
2	0.42 to 0.45	Blue
3	0.45 to 0.50	Blue
4	0.50 to 0.55	Green
5	0.55 to 0.60	Green
6	0.60 to 0.65	Red
7	0.65 to 0.70	Red
8	0.70 to 0.80	Reflected IR
9	0.80 to 0.90	Reflected IR
10	0.90 to 1.10	Reflected IR

*Combining bands 2, 4, and 7 in blue, green, and red produces a normal color image.

Water, vegetation, and urban areas are the major types of land cover and land use in the San Pablo Bay area. In Figure 1-17 the bandwidth for each multispectral image can be compared to the spectral reflectance curve for vegetation. Vegetation has a higher reflectance in the green band than in the blue and red bands where chlorophyll absorbs energy. The reflectance of vegetation increases abruptly in the reflected IR region. These spectral characteristics of vegetation are also seen in the brightness signatures of vegetated hills in the images at corresponding wavelengths. The signature of water is also different in the various spectral bands. In San Pablo Bay, patterns of suspended silt are obvious in the visible bands; in the IR bands, however, water has a uniform dark signature because these wavelengths are completely absorbed. Some of the salt evaporating ponds, identified in Figure 1-21, have red and pink signatures in Plate 1A because of red microorganisms.

Along-Track Multispectral Scanner Images Along-track multispectral scanners employ multiple linear arrays of detectors with each array recording a separate band of energy (Figure 1-19B). Because of the extended dwell time, the detector bandwidth may be narrow and produce an adequate signal. Along-track scanner images acquired by SPOT and other satellite systems are illustrated in Chapter 4.

Side-Scanning Multispectral Images Aircraft and satellite radar systems have been developed that record two or more wavelengths of microwave energy. Typical images are shown in Chapter 7.

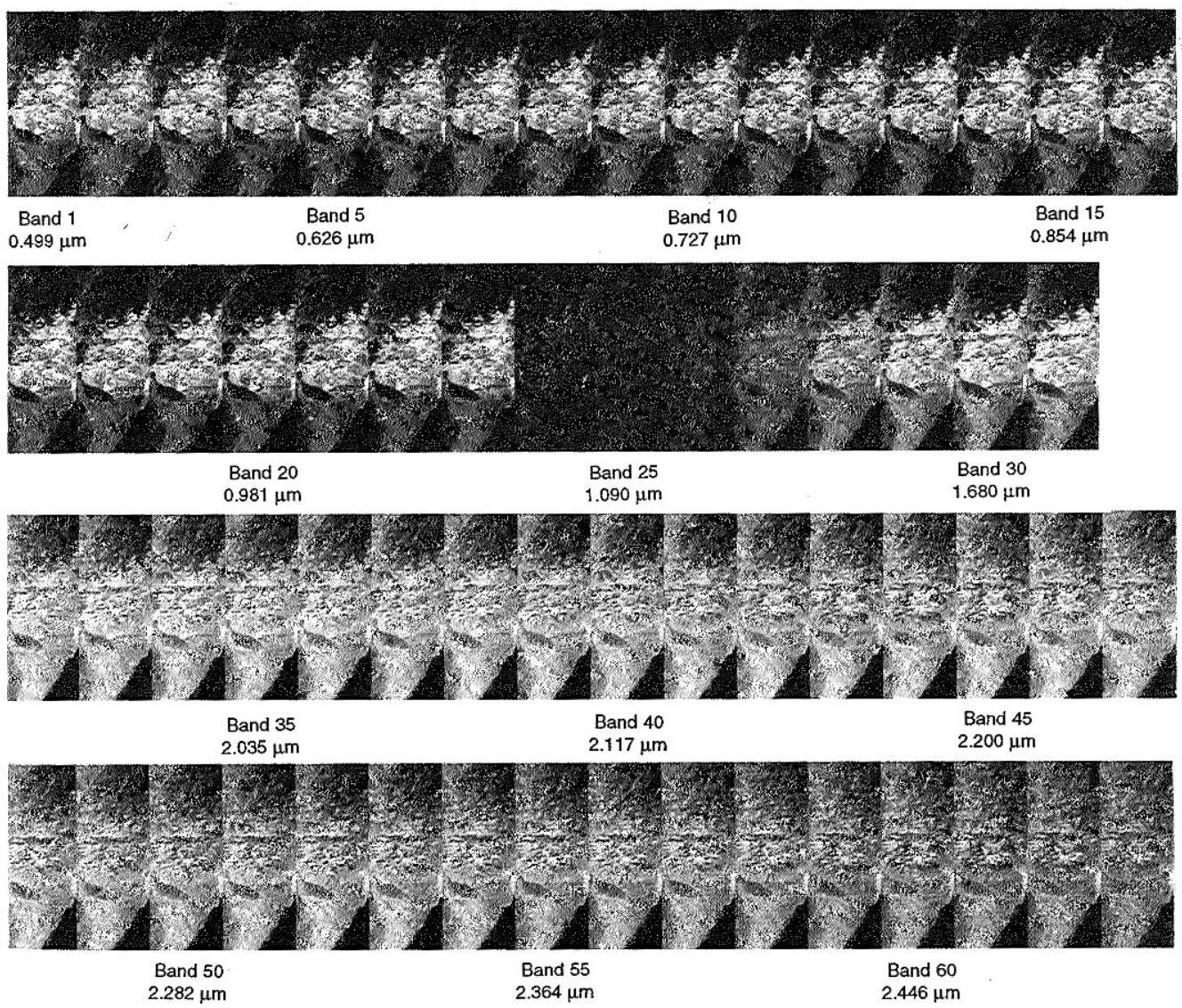

Figure 1-22 Hyperspectral scanner images of Cuprite, Nevada, acquired with a GER 63-band aircraft system.

HYPERSPECTRAL SCANNING SYSTEMS

From the beginning of remote sensing, imaging technology has advanced in two major ways:

1. Improvement in the spatial resolution of images—accomplished primarily by decreasing the *IFOV* of detectors.
2. Improvement in the spectral resolution of images—accomplished by increasing the number of spectral bands and decreasing the bandwidth of each band.

Conventional multispectral scanners record up to 10, or so, spectral bands with bandwidths on the order of 0.10 μm. *Hyperspectral scanners* are a special type of multispectral scanner that records many tens of bands with bandwidths on the order of 0.01 μm. Today these systems are used only on aircraft, but eventually they will be carried on satellites. Table 1-4 lists characteristics of some current hyperspectral scanners.

GER Hyperspectral Scanner

Figure 1-22 shows the 63 hyperspectral bands recorded by a system developed by Geophysical & Environmental Research, Incorporated (GER). The area is the Cuprite mining district in west-central Nevada (Figure 1-23). The band number and wavelength are shown for every fifth image. In Figure 1-17 the tick marks show the spectral distribution of the GER image bands. Only seven bands are located in the interval of 1.00 to 2.00 μm, which is dominated by absorption bands caused by water vapor; 24 bands are in the region of 0.50 to 1.00 μm; 32 bands are in the region of 2.00 to 2.50 μm. The poor quality of bands 24 to 28 (Figure 1-22) is due to the absorption of energy by atmospheric water vapor.

Hyperspectral images are recorded in digital format which results in a large volume of data that can be analyzed using the image-processing techniques described in Chapter 8. Daedalus Enterprises, Inc., of Ann Arbor, Michigan, also manufactures an aircraft hyperspectral scanner that records 102 bands of imagery in the visible, reflected IR, and thermal IR regions.

AVIRIS Hyperspectral Scanner

Jet Propulsion Laboratory (JPL) developed a hyperspectral scanner system called the *airborne visible/infrared imaging spectrometer* (AVIRIS), which acquires 224 images each with a spectral bandwidth of 10 nm in the region of 0.4 to 2.5 μm (Figure 1-17). AVIRIS is carried in a NASA U-2 aircraft at an altitude of 20 km. The images have a swath width of 10.5 km and a spatial resolution of 20 m (Vane and others, 1993). Plate 1B is a color image of the Cuprite mining district and was prepared from the following AVIRIS bands: The band at 2.21 μm is shown in blue, 2.138 μm in green, and 2.088 μm in red. In Figure 1-17 the spectral positions of these bands are indicated by the letters R, G, and B along the AVIRIS range. In the color image of Plate 1B the blue-gray tones are volcanic rocks that have been replaced by silica (Figure 1-23). The surrounding orange and red tones are volcanic rocks that have been replaced to various degrees by clays and other minerals. The blue tones are younger volcanic rocks that have not been replaced by other minerals. The ability to recognize replacement minerals on AVIRIS images is important for mineral exploration, as described in Chapter 11.

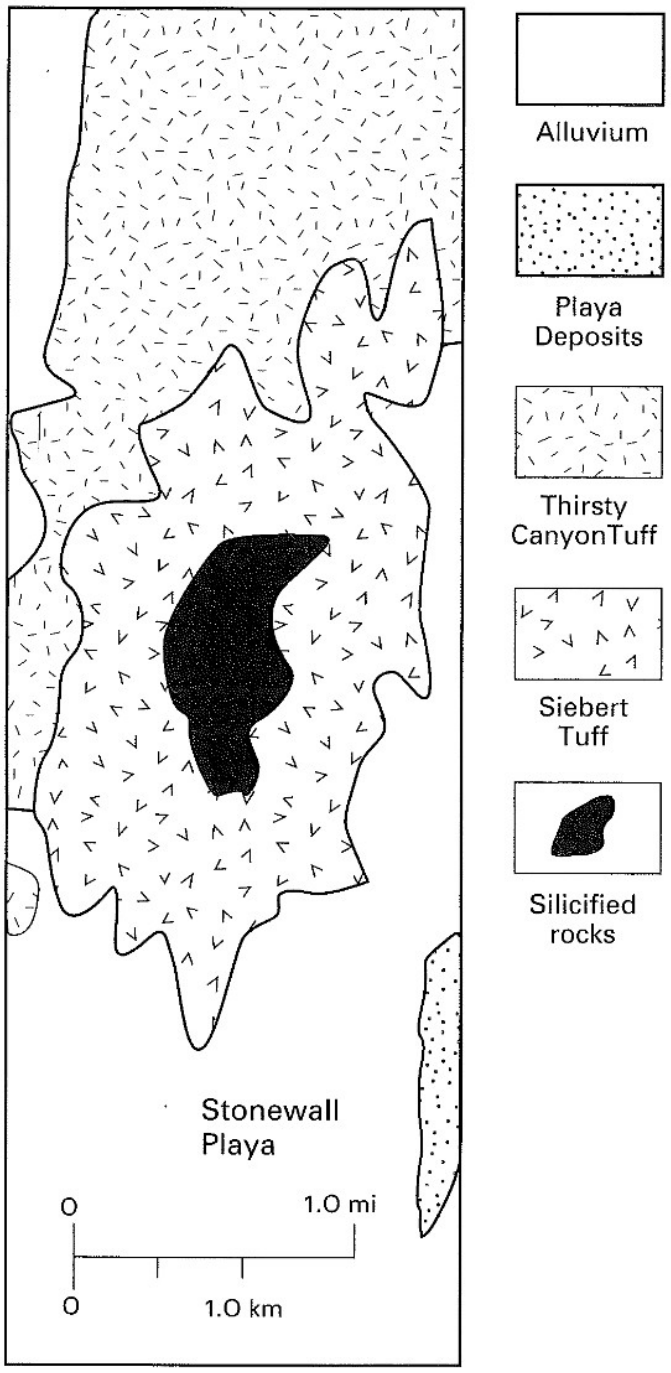

Figure 1-23 Location map of Cuprite, Nevada.

AVIRIS is currently an experimental system, but similar systems will become commercially available in the future. Specialized computer systems are required to process the large volumes of data in the 224 bands of imagery. JPL has convened a series of workshops where investigators have reported results of AVIRIS projects. Vane (1988) and Green (1990, 1991) have prepared proceedings volumes for these workshops. The journal *Remote Sensing of the Environment* devoted one issue (vol. 44, nos. 2/3, May/June, 1993) to a series of papers that describe a wide range of applications of AVIRIS images.

Reflectance Spectra from Hyperspectral Data

Hyperspectral scanners are also called *imaging spectrometers*. The narrow spectral bands of hyperspectral images may be converted into reflectance spectra (Van der Meer, 1994).

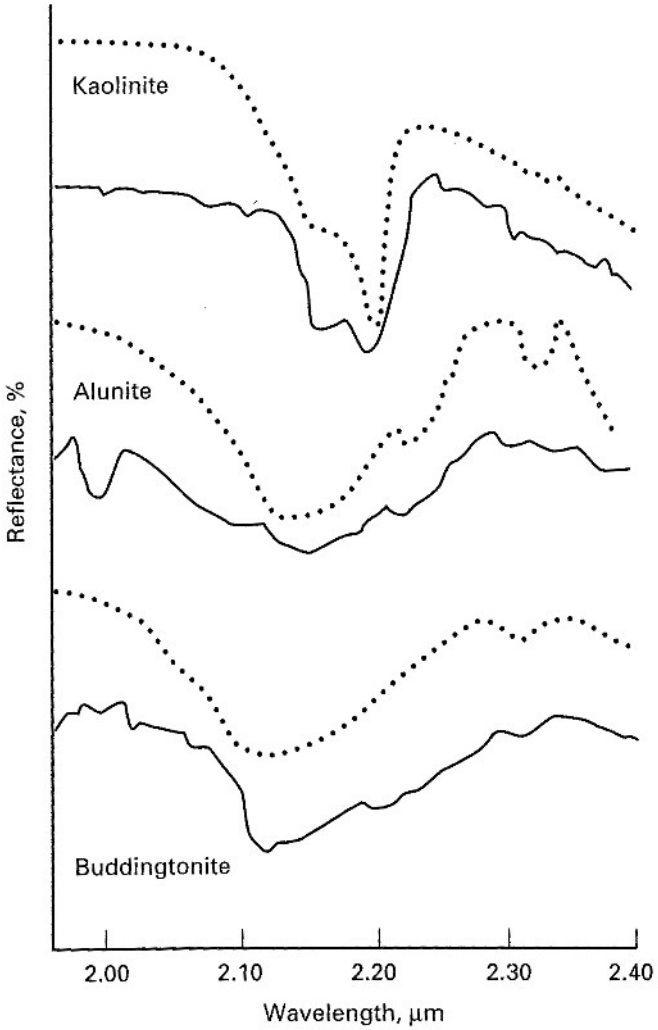

Figure 1-24 Spectra of minerals derived from AVIRIS data (solid lines) and measured by laboratory spectrometer (dotted lines). From Van de Meer (1994, Figure 3).

Figure 1-24 shows spectra that were calculated from AVIRIS data of Cuprite, Nevada. Each solid spectral curve represents an array of 5-by-5 ground resolution cells, which is an area of 100 by 100 m on the ground. The three curves represent areas where three different minerals (kaolinite, alunite, and budding-

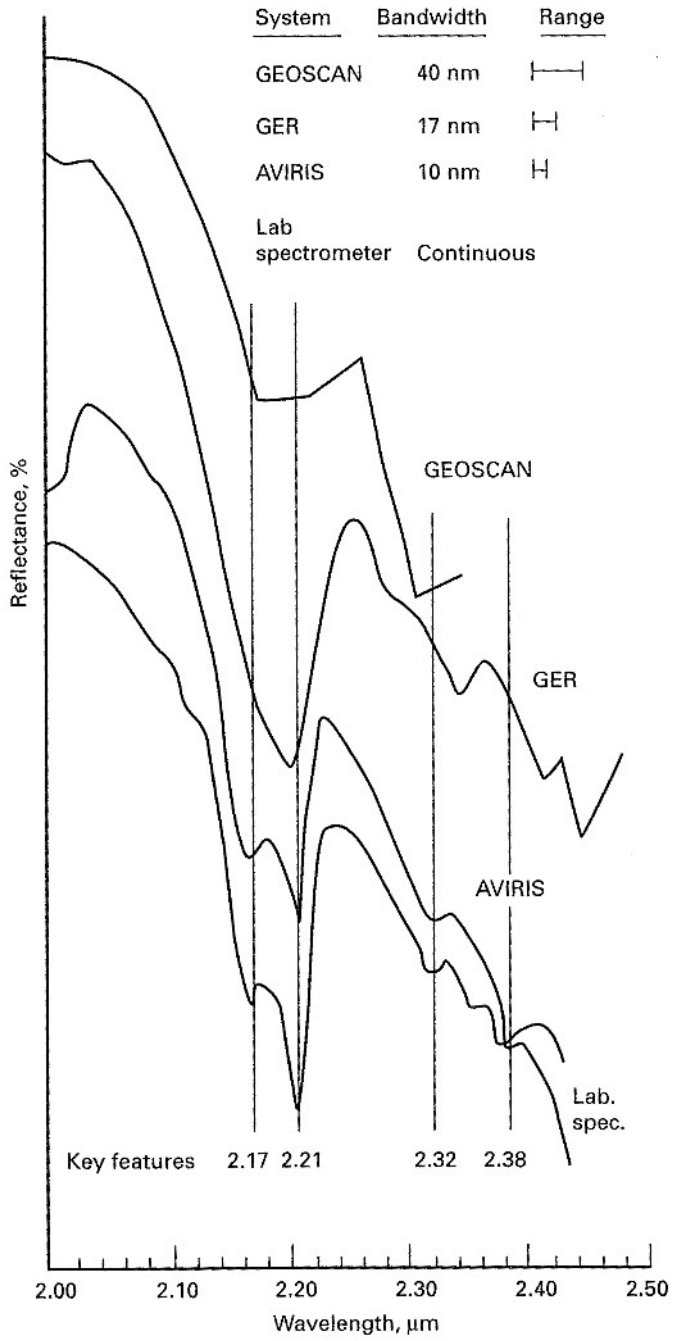

Figure 1-25 Spectra of the clay mineral kaolinite recorded by hyperspectral scanners and by a laboratory spectrometer. Bandwidths of the scanners are shown. Vertical lines indicate absorption features that are keys for recognizing the kaolinite spectrum. Compiled from data in Kruse (1996).

tonite) occur. Kaolinite is a clay mineral, alunite is aluminum sulfate, and buddingtonite is an ammonium feldspar. For each area the percentage of reflectance for each AVIRIS band is plotted as a function of wavelength. The values are connected to produce the solid curves in Figure 1-24. The dotted lines are laboratory spectra for the three minerals, which are similar to the AVIRIS spectra. The differences between the AVIRIS spectra and the spectrometer spectra are explained as follows: The ground resolution cells of AVIRIS include a variety of materials in addition to the predominant mineral, and these contaminate an AVIRIS spectrum, whereas a laboratory spectrum represents a pure sample of each mineral.

Table 1-4 lists characteristics of a Canadian along-track scanner called the SFSI, which is an acronym for SWIR (short wave IR) Full Spectrum Imager. Neville and others (1995) describe the system and show spectra and images.

Figure 1-25 shows reflectance spectra for kaolinite that were produced by Kruse (1996) from data acquired by the GER (63 bands) and AVIRIS (224 bands) hyperspectral scanners. Also shown is a spectrum from the Geoscan multispectral scanner, which records up to 24 bands that are selected from 46 available bands. Figure 1-25 lists the bandwidths of these systems and shows the bandpass range graphically. For comparison, the bottom kaolinite spectrum was recorded by a laboratory spectrometer and provides the highest spectral resolution. The vertical lines show four key absorption features from the laboratory spectrum that are diagnostic for identifying the kaolinite spectrum. Only AVIRIS, with a 10-nm bandwidth, records all the key features. Similar results were obtained for spectra of buddingtonite and alunite. Despite their lower spectral resolution, Kruse (1996) notes that the GER and Geoscan systems are useful for projects that do not require the identification of specific minerals.

In summary, the spectral resolution (bandwidth) of a remote sensing system (Figure 1-13) determines the ability to distinguish and identify materials based on their spectral characterisitics. Spatial resolution (Figure 1-14) determines the ability to distinguish objects based on their geometric characteristics.

SOURCES OF REMOTE SENSING INFORMATION

Table 1-6 lists scientific journals devoted to remote sensing that are published by technical societies or commercial publishers.

Table 1-6 Remote sensing journals and societies

Journal	*Publisher*
Canadian Journal of Remote Sensing	Canadian Aeronautics and Space Institute Saxe Building 60-75 Sparks Street Ottawa, Canada K1P 5A5
Earth Observation Magazine	EOM, Inc. 13741 E. Rice Place, Suite 125 Aurora, CO 80015
Geo Abstracts—G. Remote Sensing, Photogrammetry, and Cartography	Geo Abstracts Regency House 34 Duke Street Norwich NR3 3AP United Kingdom
Geocarto International	Geocarto International Centre G.P.O. Box 4122 Hong Kong
IEEE Transactions on Geoscience and Remote Sensing	IEEE Remote Sensing and Geoscience Society Institute of Electrical and Electronics Engineers 445 Hoes Lane Piscataway, NJ 08854
International Journal of Remote Sensing	Remote Sensing Society c/o Taylor and Francis, Ltd. Rankine Road Basingstoke, Hants. RG24 OPR United Kingdom

(concluded on the following page)

Table 1-6 *(concluded)*

Journal	*Publisher*
Photogrammetric Engineering and Remote Sensing	American Society for Photogrammetry and Remote Sensing 210 Little Falls Street Falls Church, VA 22046
Reflections	Radarsat International 3851 Shell Road, Suite 200 Richmond, BC V6X 2W2 Canada
Remote Sensing in Canada	Canadian Remote Sensing Society 130 Slater Street, Suite 818 Ottawa, Ontario K1P 6E2 Canada
Remote Sensing Newsletter	Geological Remote Sensing Group c/o Dr. Stuart Marsh British Geological Survey Keyworth, Nottingham NG12 5GG United Kingdom
Remote Sensing of Environment	Elsevier Science Publishing Company 655 Avenue of the Americas New York, NY 10010-5107
Remote Sensing Reviews	Gordon and Breach Science Publishers P.O. Box 786, Cooper Station New York, NY 10276
Washington Remote Sensing Letter	M. Felscher, Publisher P.O. Box 2075 Washington, DC 20013

Table 1-7 Remote sensing organizations and conferences.

Organization	*Address*	*Conference*
Environmental Research Institute of Michigan	P.O. Box 134001 Ann Arbor, MI 48113	"Remote Sensing of Environment" "Thematic Conferences on Remote Sensing"
EROS Data Center of U.S. Geological Survey	Sioux Falls, SD 57198	"Pecora Symposium on Remote Sensing" (annual conference)
Jet Propulsion Laboratory	4800 Oak Grove Drive Pasadena, CA 91103	Publishes reports; conducts conferences and workshops
IEEE Geoscience and Remote Sensing Society	345 East 47th Street New York, NY 10017	"IEEE International Geoscience and Remote Sensing Symposium" (annual symposium)

Table 1-8 Remote sensing images and information on Internet and the Worldwide Web

Facility	*Data*	*Address*
Canada Center for Remote Sensing	Landsat 5 and SPOT	http://www.ccrs.emr.ca/cdql/.html
EOSAT	Landsat, IRS, JERS, ERS	http://www.eosat.com
Goddard Space Flight Center	AVHRR	http://xtreme.gsfc.nasa.gov/
Japan NASDA	JERS-1	http://hdsn.eoc.nasda.go.jp/
Johnson Space Center	Images from manned satellites	http://images.jsc.nasa.gov/html/home.htm
Jet Propulsion Laboratory	Educational Outreach Center	http://www.jpl.nasa.gov/education.html
Jet Propulsion Laboratory	Imaging radar	http://southport.jpl.nasa.gov/
Jet Propulsion Laboratory	Public Information Office	http://www.jpl.nasa.gov
NASA	Starting point	http://hypatia.gsfc.nasa.gov/NASA.homepage.html
NASA	Scientific and tech. info.	http://www.sti.nasa.gov
National Oceanic and Atmospheric Administration	Image catalog	http://www.esdim.noaa.gov/NOAA.Catalog/NOAA.Catalog.html
National Oceanic and Atmospheric Administration	Weather satellite data	http://www.ncdc.noaa.gov
Radarsat Canada	Radarsat	http/radarsat.sou.gc.ca
Syracuse University	SIR-C teachers guide	http://ericir.syr.edu/NASA/nasa.htm1
U. S. Geological Survey	Global Land Information System	http://edcwww.cr.usgs.gov/glis/glis.html
U. S. Geological Survey	U.S. spy satellite images	http://edcwww.cr.usgs.gov/dclass.dclass.html
United Kingdom	Weather images	http://web/nexor.co.uk/users/jpo/weather/weather.html

Membership in these societies is open to all investigators. Cracknell (1992) has published a directory of remote sensing journals and societies that are based in Europe. In addition to these journals, many articles on remote sensing are published in journals devoted to other disciplines such as geology, geography, and oceanography. Table 1-7 lists remote sensing conferences conducted by various organizations.

Under the editorship of R. N. Colwell (1983), The American Society of Photogrammetry and Remote Sensing (ASPRS) published the second edition of the *Manual of Remote Sensing*, which is a useful reference. ASPRS is currently preparing a third edition of the manual.

Table 1-8 is a partial listing of remote sensing images and information that are accessible through Internet and the Worldwide Web. Both Internet and the Worldwide Web are dynamic environments in which new sites are being opened and existing sites are being modified or discontinued. Therefore Table 1-8 is a sample of sites that were available in early 1996.

COMMENTS

Remote sensing is defined as the science of acquiring, processing, and interpreting images and related data obtained from aircraft and spacecraft that record the interaction between matter and electromagnetic energy.

The electromagnetic spectrum is divided into wavelength regions. The regions employed in remote sensing range from short-wavelength UV energy to the long-wavelength microwave and radio energy. The electromagnetic regions are further subdivided into narrow wavelength bands. Electromagnetic energy interacts with matter by being scattered, reflected, transmitted, absorbed, or emitted. Subsequent chapters of this book describe these interactions for radiation of the different wavelength bands, together with the technology employed in sensing the radiation.

The interpretation of an image depends upon its scale, tone, texture, contrast ratio, and spatial resolution. In this text, spatial resolution refers to the minimum distance between two objects at which they can be distinguished. Remote sensing systems operate in the framing mode or the scanning mode. Multispectral images consist of two or more simultaneously recorded spectral bands of imagery. Any three bands can be combined, one each in blue, green, and red, to produce color images.

QUESTIONS

1. Use Equation 1-1 to calculate the wavelength in centimeters of radar energy at a frequency of 10 GHz. What is the frequency in gigahertz of radar energy at a wavelength of 25 cm?
2. What is the temperature of boiling water at sea level in degrees Kelvin?
3. Distinguish between the earth's radiant energy peak and the reflected energy peak.
4. The atmosphere is essential for life on earth, but it causes problems for remote sensing. Describe these problems.
5. Use Equation 1-3 to calculate the contrast ratio between a target with a brightness of 17 and a background with a brightness of 8.
6. On images acquired from a satellite (at a 910-km altitude), targets on the ground separated by 80 m can be resolved. Use Equation 1-4 to calculate the angular resolving power (in milliradians) of the scanning system.
7. Assume that your eyes have the normal resolving power (0.2 mrad) and that you are an airline passenger at an altitude of 9 km. For targets on the ground with high contrast ratio, what is the minimum separation (in meters) at which you can resolve these targets?
8. An airborne cross-track scanner has the following characteristics: *IFOV* = 1.5 mrad; angular field of view = 45°; scan mirror rotates at 4000 rpm (revolutions per minute). The aircraft altitude is 10 km. Calculate the following:
   Size of ground resolution cell = ____ by ____ m
   Width of ground swath = ____ km
   Dwell time for a ground resolution cell = ____ sec.
9. An along-track scanner has detectors with a 2-mrad *IFOV*. The scanner is carried in an aircraft at an altitude of 15 km and a ground speed of 600 km · h^{-1}. Calculate the following:
   Ground resolution cell = ____ by ____ m
   Dwell time for a ground resolution cell = ____ sec.
10. Refer to the aircraft multispectral scanner images and map of San Pablo Bay (Figures 1-20, 1-21). Select the three images that show maximum differences in brightness (reflectance) for the following terrain categories:
    Vegetation in northeast corner of the scene: bands ____, ____, ____.
    Silty water in San Pablo Bay adjacent to Mare Island: bands ____, ____, ____.
    Urban areas of Vallejo: bands ____, ____, ____.
    Salt ponds in northwest portion of the image: bands ____, ____.

REFERENCES

Clark, R. N., and others, 1990, High spectral resolution reflectance spectroscopy of minerals: Journal of Geophysical Research, v. 95, p. 12,653–12,680.

Colwell, R. N., ed., 1983, Manual of remote sensing, second edition: American Society of Photogrammetry, Falls Church, VA.

Cracknell, A. P., 1992, Learned societies, learned journals and other publications: International Journal of Remote Sensing, v. 13, p. 1217–1228.

Fischer, W. A. and others, 1975, History of remote sensing *in* Reeves, R. G., ed., Manual of remote sensing: ch. 2, p. 27–50, American Society of Photogrammetry, Falls Church, VA.

Forshaw, M. R., A. Haskell, P. F. Miller, D. J. Stanley, and J. R. G. Townshend, 1983, Spatial resolution of remotely sensed imagery—a review paper: International Journal Remote Sensing, v. 4, p. 497–520.

Green, R. O., 1990, Proceedings of the second Airborne Visible/Infrared Imaging Spectrometer (AVIRIS) workshop: Jet Propulsion Laboratory Publication 90-54, Pasadena, CA.

Green, R. O., 1991, Proceedings of the third Airborne Visible/Infrared Imaging Spectrometer (AVIRIS) workshop: Jet Propulsion Laboratory Publication 91-28, Pasadena, CA.

Gregory, R. L., 1966, Eye and brain, the psychology of seeing: World University Library, McGraw-Hill Book Co., New York, NY.

Grove, C. I., S. J. Hook, E. D. Paylor, 1992, Laboratory reflectance spectra of 150 minerals, 0.4 to 2.5 micrometers: Jet Propulsion Laboratory Publication 92-2, Pasadena, CA.

Hunt, G. L., 1980, Electromagnetic radiation—the communication link in remote sensing, *in* Siegal, B. S., and Gillespie, A. R., eds., Remote sensing in geology: John Wiley & Sons, New York, NY.

King, D. L., 1995, Airborne multispectral digital camera and video sensors—a critical review of system designs and applications: Canadian Journal of Remote Sensing, v. 21, p. 245–273.

Kruse, F. A., 1996, Cuprite Nevada—supplemental field trip information, *in* Shaulis, L., ed., Remote sensing field trip of Red Rock Canyon, Death Valley, Goldfield, and Cuprite: Eleventh Thematic Conference on Applied Geologic Remote Sensing, Environmental Research Institute of Michigan, Ann Arbor, MI.

Longshaw, T. G., 1976, Application of an analytical approach to field spectroscopy in geological remote sensing: Modern geology, v. 5, p. 93–107.

Lowman, P. D., 1969, Apollo 9 multispectral photography—geologic analysis: NASA Goddard Space Flight Center, Report X-644-69-423, Greenbelt, MD.

Marsh, S. E., J. L. Walsh, C. T. Lee, and L. A. Graham, 1991, Multitemporal analysis of hazardous waste sites through the use of a new bi-spectral video remote sensing system and standard color-IR photography: Photogrammetric Engineering and Remote Sensing, v. 57, p. 1221–1226.

Marsh, S. E., J. L. Walsh, and C. Sobrevila, 1994, Evaluation of airborne video data for land-cover classification accuracy assessment in an isolated Brazilian forest: Remote sensing of environment, v. 48, p. 61–69.

McKinney, R. G., 1980, Photographic materials and processing *in* Slama, C. C. , ed., Manual of photogrammetry, fourth edition: ch. 6, p. 305–366, American Society of Photogrammetry, Falls Church, VA.

Monday, H. M., J. S. Urban, D. Mulawa, and C. A. Benkelman, 1994, City of Irving utilizes high resolution multispectral imagery for N. P. D. E. S. compliance: Photogrammetric Engineering and Remote Sensing, v. 60, p. 411–416.

NASA, 1977, Skylab explores the earth: NASA SP-250, Washington, DC.

Neale, C. M. U. and B. G. Crowther, 1994, An airborne multispectral video/radiometer remote sensing system—development and calibration: Remote Sensing of Environment, v. 49, p. 187–194.

Neville, R. A., N. Rowlands, R. Marois, and I. Powell, 1995, SFSI—Canada's first airborne SWIR imaging spectrometer: Canadian Journal of Remote Sensing, v. 21, p. 328–336.

Price, J. C., 1994, How unique are spectral signatures?: Remote Sensing of Environment, v. 49, p. 181–186.

Price, J. C., 1995, Examples of high resolution visible to near-infrared reflectance spectra and a standardized collection for remote sensing studies: International Journal of Remote Sensing, v. 16, p. 993–1000.

Rosenberg, P., 1971, Resolution, detectability, and recognizability: Photogrammetric Engineering, v. 37, p. 1244–1258.

Slater, P. N., 1983, Photographic systems for remote sensing *in* Colwell, R. N., ed., Manual of remote sensing, second edition: ch. 6, p. 231–291, American Society Photogrammetry, Falls Church, VA.

Slater, P. N., 1985, Survey of multispectral imaging systems for earth observation, in R. N. Colwell, ed., Manual of remote sensing, second edition: ch. 6, p. 231–291, American Society for Photogrammetry and Remote Sensing, Falls Church, VA.

Suits, G. H., 1983, The nature of electromagnetic radiation *in* Colwell, R. N., ed., Manual of remote sensing, second edition: ch. 2, p. 37–60, American Society of Photogrammetry, Falls Church, VA.

Van der Meer, F., 1994, Extraction of mineral absorption features from high-spectral resolution data using non-parametric geostatistical techniques: International Journal of Remote Sensing, v. 15, p. 2193–2214.

Vane, G., ed., 1988, Proceedings of the Airborne Visible/Infrared Imaging Spectrometer (AVIRIS) performance evaluation workshop: Jet Propulsion Laboratory Publication 88-38, Pasadena, CA.

Vane, G., R., O. Green, T. G. Chrien, H. T. Enmark, E. G. Hansen, and W. M. Porter, 1993, The Airborne Visible/Infrared Imaging Spectrometer (AVIRIS): Remote Sensing of Environment, v. 44, p. 127–143.

ADDITIONAL READING

Avery, T. E. and G. L. Berlin, 1992, Fundamentals of remote sensing and airphoto interpretation, fifth edition: Macmillan, New York, NY.

Beaumont, E. A. and Foster, N. H., eds., 1992, Remote sensing: American Association of Petroleum Geologists, Treatise of Petroleum Geology Reprint Series, no. 19, Tulsa, OK.

Ben-Dor, E. and F. A. Kruse, 1995, Surface mineral mapping of Makhtesh Ramon Negev, Israel using GER 63 channel scanner data: International Journal of Remote Sensing, v. 16, p. 3529–3553.

Colwell, R. N. and others, 1963, Basic matter and energy relationships involved in remote reconnaissance: Photogrammatric Engineering and Remote Sensing, v. 29, p. 761–799.

Elachi, C., 1987, Introduction to the physics and techniques of remote sensing: John Wiley & Sons, New York, NY.

Everitt, J. H., and others, 1995, A three-camera multispectral digital video imaging system: Remote Sensing of Environment, v. 54, p. 333–337.

Hook, S. J., C. D. Elvidge, M. Rast, and H. Watanabe, 1991, An evaluation of short-wavelength-infrared (SWIR) data from the AVIRIS and GEOSCAN instruments for mineralogic mapping at Cuprite, Nevada: Geophysics, v. 56, p. 1432–1440.

Hyatt, E., 1988, Keyguide to information sources in remote sensing: Mansell, London, England.

Lillesand, T. M. and R. W. Kiefer, 1994, Remote sensing and image interpretation, third edition: John Wiley & Sons, New York, NY.

Rees, W. G., 1990, Physical principles of remote sensing: Cambridge University Press, Cambridge, England.

Southworth, C. S., 1985, Characteristics and availability of data from earth imaging satellites: U.S. Geological Survey, Bulletin 1631.

Vane, G., ed., 1990, Imaging spectroscopy of the terrestrial environment: SPIE—The International Society for Optical Engineering, v. 1298.

Vane, G. and A. F. H. Goetz, 1993, Terrestrial imaging spectrometry—current status, future trends: Remote Sensing of Environment, v. 44, p. 117–126.